($n = 3$) could not be clearly determined. For the para-aortic lymph nodes, 24 patients were positive and 86 patients were negative. There were 36 patients (32%) in stage I, 15 patients (14%) in stage II, and 54 patients (50%) in stage III according to the FIGO staging. Five patients (4%) could not be staged because of insufficient FIGO staging information. Endometrioid adenocarcinoma, with 84 patients (76%), was the most frequent histological type encountered. Six other types were detected with considerably fewer frequencies. The histological types for two patients were not described in their medical records.

Among the cases not receiving postoperative chemotherapy, just the whole pelvis was irradiated in 86 cases (78%) and the para-aortic lymph node area plus the whole pelvis were irradiated in 24 cases (22%). As for the cases with postoperative chemotherapy, the CAP regimen was used in 32 cases (29%) and the TC regimen in 14 cases (13%).

To account for the high risk of local recurrence after surgery, a strong primary possibility was deep invasion in over 50% in 80 patients (82%) (Table 1). Secondarily, there were positive lymph node metastases in 36 patients (34%) (Table 1). Other reasons were ovarian invasion in five patients and cervical invasion in one patient. PORT was performed even for four patients with FIGO stage IA or IB with high risk of local recurrence. The reasons were histological FIGO grade 3 in three patients, and adenosquamous carcinoma in one patient. Although the intermediate low-risk group was not a target of PORT, two patients with intermediate low risk were given PORT because the residual lesions were strongly doubted by the surgeon in spite of negative histopathology.

Survival

The median follow-up time for all patients was 59.2 months (range; 6.5–235.2 months). The number of survivors at the end of the observation period was 93 (84%), and the number of disease-free survivors was 81 (73%). The OS rate at 5 years was 84%, and the DFS rate at 5 years was 77% for all patients. Both OS and DFS reached a plateau at approximately 3 years. Patients younger than 60 years had significantly better OS (log–rank $P = 0.044$, odds ratio [OR] = 0.383, and 95% confidence interval [CI] = 0.145–1.008) and DFS (log–rank $P = 0.013$, OR = 0.389, and 95%CI = 0.180–0.840) than patients 60 years or older (Fig. 1). Moreover, when limited to the histological type of endometrioid adenocarcinoma ($n = 84$), there was a significant difference in DFS between patients 60 years or older, and those

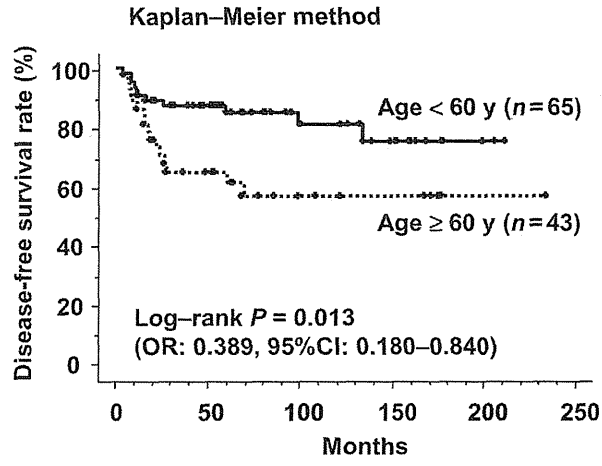

Figure 1 Disease-free survival curves by age (less than 60 years old vs 60 years or older). CI, confidence interval; OR, odds ratio.

under 60 years old (log–rank $P = 0.004$, OR = 0.289, and 95%CI = 0.119–0.703). However, when the age was raised to 65 years, the earlier significant difference in DFS shown for those younger than 60 years vanished ($P = 0.067$). When the age was raised to 70 years, there was a significant difference in DFS ($P = 0.0030$, OR = 0.274, and 95%CI = 0.109–0.685). The numbers of patients aged ≥65 and 70 years old were 25 (23%) and 10 (9%), respectively.

Certain prognostic factors (as determined by univariate analysis, Table 1) for both OS and DFS were examined. Pathological stage, with or without lymph node metastasis, and with or without chemotherapy, and age were studied. The 5-year OS and DFS rates were 93% and 87% in FIGO pathological stage I cases, 85% and 79% in stage II cases, and 83% and 74% in stage III cases, respectively. A significantly higher DFS rate in stage I ($n = 36$) emerged when compared with stages II–III ($n = 69$) (log–rank $P = 0.040$). Significant differences for DFS were not shown for those with and without lymph node metastasis (log–rank $P = 0.15$) and with and without postoperative chemotherapy (log–rank $P = 0.13$). However, for those with and without para-aortic lymph node metastasis the difference was significant (log–rank $P = 0.0006$, OR = 0.285, 95%CI = 0.133–0.612) (Table 1).

On multivariate analysis (Table 2), poor DFS correlated only with age ≥ 60 years ($P = 0.035$).

The distribution of variables according to age (age <60 vs age ≥60) is summarized in Table 3. There were significantly more cases of endometrioid

Table 2 Multivariate analysis of disease-free survival

Factor	*P*-value	OR	95%CI
Age			
<60 y	0.035	0.427	0.193–0.944
≥60 y			
PALN			
(−)	0.067	0.451	0.192–1.058
(+)			
FIGO stage			
I	0.18	0.484	0.167–1.405
II–III			

CI, confidence interval; FIGO, International Federation of Gynecology and Obstetrics; OR, odds ratio; PALN, para-aortic lymph node.

adenocarcinoma on histological type ($P = 0.019$) and fewer high-risk cases ($P = 0.017$) in patients ≥60 years old than in patients <60 years old.

Complications

According to the CTCAE v3.0, lower limb edema, intestinal obstruction, and diarrhea were adverse events of grade 3 or more. Regarding complications of grade 3 or more, lower limb edema was seen in 16 patients (14%), intestinal obstruction was seen in nine patients (8%), and diarrhea was seen in three patients (3%). In this study, lower limb edema was recorded in 15 patients with grade 1 complications and 13 patients with grade 2 complications. There was no grade 3 or 4 myelosuppression in any of the cases.

Discussion

In this retrospective study of endometrial cancer in our institution, prognostic factors were evaluated in endometrial cancer patients and were focused particularly on the effect of advanced age on the outcome of surgery and PORT. The limitations of our study included the retrospective nature of the study and the heterogeneity of the patient population in the two arms (<60 years vs ≥60 years).

In a prospective randomized trial of postoperative radiation therapy in endometrial carcinoma (PORTEC) for stage I disease, Creutzberg *et al.*[13] reported that patient age ≥60 years was an independent predictor of death from endometrial carcinoma (hazard ratio of 3.1 and 95%CI , 1.2–8; $P = 0.02$). The data in the literature also suggest that there is an incremental increase in the risk of dying from endometrial carcinoma with increasing age. In a review of 819 patients with stage I–II endometrial carcinoma from the Gynecologic Oncology Group database, Zaino *et al.* demonstrated that the relative risk (RR) increased from 1.0 for patients who were aged ≤45 years (reference) at the time of diagnosis to 2.0 for patients aged 55 years, to 3.4 for patients aged 65 years, and to 4.7 for patients aged ≥75 years.[2] According to Alektiar *et al.*,[12] patient age ≥70 years was found to be an independent predictor of poor locoregional control (RR: 3 and 95%CI , 1–10; $P = 0.019$), DFS (RR: 2 and 95%CI , 1–13; $P = 0.03$), and OS (RR: 4 and 95%CI , 2–7; $P = 0.001$). Jolly *et al.*[14] concluded from a retrospective study that older endometrial cancer (age >63 years) patients had a significantly decreased OS, cause-specific survival, and greater risk of recurrence following PORT that were independent of other prognostic factors and/or treatment technique. According to Lee *et al.*,[15] their study ($n = 51\,471$) of a large population of uterine cancer patients demonstrated that those 40 years or younger have an OS advantage compared with women older than 40 years, independent of other clinicopathological prognosticators. Farley *et al.*[16] concluded that age (older than 50) is a specific and significant predictor of outcome in endometrioid adenocarcinoma of the uterus ($n = 328$). The frequent association between older age in endometrial carcinoma patients on the one hand and deep myometrial invasion and aggressive histologies always raises the possibility that the poor outcome in older patients is entirely the result of such an association. Why older patients with early-stage endometrial carcinoma tend to fare worse independent of other factors is not clear. Nevertheless, clinical efforts should be directed toward maximizing the therapeutic ratio in those patients. The notion of limited life expectancy should not hinder that effort because survival to the age of 80 years and beyond has been reported to have increased in many developed countries.[17] The remaining life expectancy of a white US woman aged 75 years is estimated to be 11.7 years.[18]

The treatment methods were changed for postoperative adjuvant therapy in our institution due to a pathological result after operation. Seeing the treatment outcome, the 5-year DFS rate of each FIGO stage was 82% in stage I, 79% in stage II, and 74% in stage III. These outcomes are comparable to other institutions. In the gynecology tumor committee report of 1993 in Japan,[19] the OS rate for five years was 84.0% in stage I, 73.5% in stage II, and 54.8% in stage III. As for our outcome results, only those cases receiving PORT in our department were evaluated, and it is likely that the results would show further improvement for stage I if the patients in the low-risk group were included. There

Table 3 Distribution of variables according to age

Variables	<60 years	($n = 67$)	≥60 years	($n = 43$)	*P*-value (×2)
PLN					
(+)	21	(41%)	15	(27%)	0.96
(−)	30	(59%)	41	(73%)	
PALN					
(+)	15	(23%)	9	(20%)	0.67
(−)	50	(77%)	36	(80%)	
FIGO stage					
I	20	(33%)	16	(36%)	0.65
II–III	41	(67%)	28	(64%)	
Histological type					
EA	43	(69%)	41	(89%)	0.019
not EA	19	(31%)	5	(11%)	
FIGO grade					
1	25	(50%)	16	(47%)	0.81
2	14	(28%)	11	(32%)	
3	11	(22%)	7	(21%)	
Risk group					
High	51	(80%)	25	(57%)	0.017
Intermediate–high	12	(19%)	18	(41%)	
Intermediate–low	1	(1%)	1	(2%)	
Chemotherapy					
With	30	(49%)	16	(37%)	0.21
Without	31	(51%)	27	(63%)	
Depth					
a–b†	10	(19%)	8	(18%)	0.27
c–d‡	44	(81%)	36	(82%)	

†<50% myometrial invasion. ‡>50% myometrial invasion. DFS, disease-free survival; EA, endometrioid adenocarcinoma; FIGO, International Federation of Gynecology and Obstetrics; OS, overall survival; PALN, para-aortic lymph node; PLN, pelvic lymph node.

were only 15 examples for stage II, and the number of cases might not be sufficient to analyze treatment results. On the other hand, there were 55 examples of stage III, which constitutes an excellent OS rate. A phase III randomized trial showed improved survival with the use of chemotherapy for stage III and IV endometrial cancer.[20,21] However, pelvic and abdominal failure rates were alarmingly high, which appears to be persuasive for the integration of radiation and chemotherapy as performed in our institution.

According to our multivariate analysis of DFS, being a senior citizen is in itself an independent risk factor. More intensive treatment may be necessary for senior citizens than for young people. A total dose of approximately 50 Gy in PORT has already been prescribed, and because any further dose increase is difficult, the inclusion of postoperative chemotherapy can be expected. According to a recent Japanese Gynecologic Oncology Group study,[22] adjuvant CAP chemotherapy may be a useful alternative to PORT for intermediate-risk endometrial cancer. Moreover, adjuvant vaginal high-dose-rate brachytherapy alone may be a safe and effective alternative to pelvic external beam PORT for surgical early stage endometrial cancer.[23,24]

References

1. Kosary CL. FIGO stage, histology, histologic grade, age and race as prognostic factors in determining survival for cancers of the female gynecological system: An analysis of 1973–1987 SEER cases of cancers of the endometrium, cervix, ovary, vulva, and vagina. *Semin Surg Oncol* 1994; **10**: 31–46.
2. Zaino RJ, Kurman RJ, Diana KL, Morrow CP. Pathologic models to predict outcome for women with endometrioid adenocarcinoma: The importance of the distinction between surgical stage and clinical stage – a Gynecologic Oncology Group study. *Cancer* 1996; **77**: 1115–1121.
3. Abeler VM, Kjørstad KE. Endometrial adenocarcinoma in Norway. A study of a total population. *Cancer* 1991; **67**: 3093–3103.
4. Irwin C, Levin W, Fyles A, Pintilie M, Manchul L, Kirkbride P. The role of adjuvant radiotherapy in carcinoma of the endometrium: results in 550 patients with pathologic stage I disease. *Gynecol Oncol* 1998; **70**: 247–254.

5. Poulsen MG, Roberts SJ. Prognostic variables in endometrial carcinoma. *Int J Radiat Oncol Biol Phys* 1987; **13**: 1043–1052.
6. Mundt AJ, Waggoner S, Yamada D, Rotmensch J, Connell PP. Age as a prognostic factor for recurrence in patients with endometrial carcinoma. *Gynecol Oncol* 2000; **79**: 79–85.
7. Grigsby PW, Perez CA, Kuten A *et al.* Clinical stage I endometrial cancer: Prognostic factors for local control and distant metastasis and implications of the new FIGO surgical staging system. *Int J Radiat Oncol Biol Phys* 1992; **22**: 905–911.
8. Lindahl B, Ranstam J, Willén R. Five year survival rate in endometrial carcinoma stages I-II: Influence of degree of tumour differentiation, age, myometrial invasion and DNA content. *Br J Obstet Gynaecol* 1994; **101**: 621–625.
9. Alektiar KM, McKee A, Venkatraman E *et al.* Intravaginal high-dose-rate brachytherapy for Stage IB (FIGO Grade 1, 2) endometrial cancer. *Int J Radiat Oncol Biol Phys* 2002; **53**: 707–713.
10. Samet J, Hunt WC, Key C, Humble CG, Goodwin JS. Choice of cancer therapy varies with age of patient. *JAMA* 1986; **255**: 3385–3390.
11. Schrag D, Cramer LD, Bach PB, Begg CB. Age and adjuvant chemotherapy use after surgery for stage III colon cancer. *J Natl Cancer Inst* 2001; **93**: 850–857.
12. Alektiar KM, Venkatraman E, Abu-Rustum N, Barakat RR. Is endometrial carcinoma intrinsically more aggressive in elderly patients? *Cancer* 2003; **98**: 2368–2377.
13. Creutzberg CL, Van Putten WL, Koper PC *et al.* Surgery and postoperative radiotherapy versus surgery alone for patients with stage-1 endometrial carcinoma: Multicentre randomized trial. PORTEC Study Group. Post Operative Radiation Therapy in Endometrial Carcinoma. *Lancet* 2000; **355**: 1404–1411.
14. Jolly S, Vargas CE, Kumar T *et al.* The impact of age on long-term outcome in patients with endometrial cancer treated with postoperative radiation. *Gynecol Oncol* 2006; **103**: 87–93.
15. Lee NK, Cheung MK, Shin JY *et al.* Prognostic factors for uterine cancer in reproductive-aged women. *Obstet Gynecol* 2007; **109**: 655–662.
16. Farley JH, Nycum LR, Birrer MJ, Park RC, Taylor RR. Age-specific survival of women with endometrioid adenocarcinoma of the uterus. *Gynecol Oncol* 2000; **79**: 86–89.
17. Manton KG, Vaupel JW. Survival after the age of 80 in the United States, Sweden, France, England, and Japan. *N Engl J Med* 1995; **333**: 1232–1235.
18. Taeuber CM. Sixty-five plus in America. Current Population Reports. Special Studies. Washington, DC: US Department of Commerce, Economics and Statistics Administration, Bureau of the Census, 1996; publication no. P23–173RV.
19. The Cancer Committee of the Japan Society of Gynecology. [The 41st treatment annual report. 5-year result of treatment started in 1993 for cervical and endometrial carcinoma.] *J Jpn Soc Obstet Gynecol* 2008; **60**: 1876–1901. (In Japanese.)
20. Randall ME, Brunetto VL, Muss H. Whole abdominal radiotherapy versus combination doxorubicin-cisplatin chemotherapy in advanced endometrial carcinoma: A randomized phase III trial of the Gynecologic Oncology Group. *Proc Am Soc Clin Oncol* 2003; **22**: 2.
21. Randall ME, Spirtos NM, Dvoretsky P. Whole abdominal radiotherapy versus combination chemotherapy with doxorubicin and cisplatin in advanced endometrial carcinoma (phase III): Gynecologic Oncology Group Study no. 122. *J Natl Cancer Inst Monogr* 1995; **19**: 13–15.
22. Susumu N, Sagae S, Udagawa Y *et al.* Japanese Gynecologic Oncology Group.Randomized phase III trial of pelvic radiotherapy versus cisplatin-based combined chemotherapy in patients with intermediate- and high-risk endometrial cancer: A Japanese Gynecologic Oncology Group study. *Gynecol Oncol* 2008; **108**: 226–233.
23. Jolly S, Vargas C, Kumar T *et al.* Vaginal brachytherapy alone: An alternative to adjuvant whole pelvis radiation for early stage endometrial cancer. *Gynecol Oncol* 2005; **97**: 887–892.
24. Solhjem MC, Petersen IA, Haddock MG. Vaginal brachytherapy alone is sufficient adjuvant treatment of surgical stage I endometrial cancer. *Int J Radiat Oncol Biol Phys* 2005; **62**: 1379–1384.

Med Oncol
DOI 10.1007/s12032-010-9511-6

ORIGINAL PAPER

Aromatase inhibitor anastrozole as a second-line hormonal treatment to a recurrent low-grade endometrial stromal sarcoma: a case report

Keiko Shoji · Katsutoshi Oda · Shunsuke Nakagawa · Kei Kawana · Toshiharu Yasugi · Yuji Ikeda · Yutaka Takazawa · Shiro Kozuma · Yuji Taketani

Received: 18 January 2010 / Accepted: 17 March 2010

Abstract Low-grade endometrial stromal sarcoma (ESS) is a rare neoplasm and is generally an indolent tumor with estrogen and progesterone receptors. Objective responses by hormonal treatment with progestin or aromatase inhibitor have been reported, however, long-term management of this disease could be difficult if it becomes refractory to one of these hormonal therapies. A 34-year-old woman was diagnosed with stage I low-grade ESS at the time of hysterectomy for presumed uterine fibroma. Five years later, she recurred with multiple tumors in the lower abdomen. After an optimal surgery, she was free from progression for 6 years with progestin treatment (medroxyprogesterone acetate: MPA, 200–600 mg daily). Thereafter, she recurred twice during the MPA treatment and received debulking surgery each time. MPA was discontinued at age of 53, because another recurrent tumor grew up to 13 cm in diameter. Aromatase inhibitor anastrozole was then given at a daily dose of 1 mg with partial response (the tumor size decreased to 7 cm in diameter) for a duration of 9 months. After complete resection of the recurrent tumor, she remains progression-free for 16 months. Anastrozole was effective to recurrent low-grade ESS even after being refractory to progestin therapy. Aromatase inhibitor treatment may be a useful option as a second-line hormonal treatment to low-grade ESS.

K. Shoji · K. Oda (✉) · S. Nakagawa · K. Kawana · T. Yasugi · Y. Ikeda · S. Kozuma · Y. Taketani
Department of Obstetrics and Gynecology, Faculty of Medicine, The University of Tokyo, 7-3-1 Hongo Bunkyo-ku, Tokyo 113-8655, Japan
e-mail: katsutoshi-tky@umin.ac.jp

Y. Takazawa
Department of Pathology, Faculty of Medicine, The University of Tokyo, 7-3-1 Hongo Bunkyo-ku, Tokyo 113-8655, Japan

Published online: 31 March 2010

Keywords Low-grade endometrial stromal sarcoma · Uterine corpus · Recurrence · Aromatase inhibitor · Progestin therapy · Hormonal treatment

Introduction

Endometrial stromal sarcoma (ESS) is a rare neoplasm, accounting for 0.2% or less of gynecologic malignancies [1]. Low-grade ESS usually expresses estrogen receptors (ER) and progesterone receptors (PR), and estrogen acts as a growth stimulus [2, 3]. Objective responses have been obtained with progestin therapy, such as megestrol acetate and medroxyprogesterone acetate (MPA) [4, 5]. More recently, the efficacy of a non-steroid aromatase inhibitor has been also reported [6, 7], as it inhibits estrogen synthesis. Although either type of hormonal therapy might be useful as a first-line therapy, it is still uncertain whether a second-line hormonal treatment is effective to repetitively recurrent ESS with resistance to a first-line therapy.

We report a case of recurrent low-grade ESS with long-term survival, treated with MPA for 13 years as a first line and aromatase inhibitor anastrozole for 9 months as a second-line hormonal therapy.

Case report

A 34-year-old woman (gravida 4, para 2) underwent a total abdominal hysterectomy for presumed uterine fibroma at her local hospital in 1988. The histopathological result revealed stage I low-grade ESS of the corpus uteri. In December 1993, she was referred to our hospital, and a computed tomography (CT) scan revealed a 9-cm pelvic mass, bilateral ovarian masses (4 cm on the left and 7 cm

on the right), and para-aortic lymph node enlargement. She underwent secondary debulking surgery, including bilateral salpingo-oophorectomy, omentectomy, bowel resection, and biopsy of para-aortic lymph nodes. All the residual tumors were less than 1 cm in diameter. The final pathology revealed recurrence of the low-grade ESS (Fig. 1a), involving the bilateral adnexae, ileum, appendix, colon, omentum, and para-aortic lymph nodes. Immunohistochemical analysis showed a strong nuclear staining for both ER and PR (Fig. 1b, c), as well as CD10 (Fig. 1d) and vimentin, and a negative staining for HHF35, 1A4, Desmin, and CD34. Postoperatively, she was started on MPA at a daily dose of 600 mg. Three years after the MPA therapy, complete response was pathologically confirmed by second look laparoscopy. MPA was continued at a daily dose of 200–400 mg without any appreciable adverse effects.

In April 2000, surgical biopsy of a 2-cm mass around the liver confirmed the recurrence of the disease on peritoneum. Two years later, she received another debulking procedure with partial liver resection for a 5-cm tumor and resection of another 5-cm pelvic tumor. After the surgery, she was hospitalized four times within 2 years due to grade 2 ileus. In June 2006, a CT scan showed a 5-cm solid mass in the left upper quadrant. The patient did not choose a debulking surgery and was kept treated with MPA at a daily dose of 200–400 mg. Eight months later, she was found to have progression of disease, represented by enlargement of the mass up to 13 cm in diameter and appearance of 4 cm mesenteric mass in the pelvis (Fig. 2a). Then, MPA treatment was discontinued, and anastrozole at a daily dose of 1 mg was started with an informed consent. After 9 months of the treatment, the tumor in the left upper quadrant was decreased to 7 cm in diameter and the mesenteric tumor was undetected (Fig. 2b). Anastrozole was discontinued because of arthritis with grade 2 joint-function disorder. Then, she underwent complete resection of the recurrent tumor. Pathological findings also revealed the significant effect of anastrozole. As shown in Fig. 3, the majority of the tumor cells was necrotic and replaced by numerous foamy histiocytes. The viable cells remained partly in the marginal lesion with expression of ER and PR. She recovered from the joint-function disorder shortly after the surgery and remains asymptomatic and progression-free for 16 months.

Discussion

ESS is subdivided histopathologically into low-grade and undifferentiated (or high-grade) forms depending on the morphology, number of mitoses, cellularity, and necrosis. The primary treatment for low-grade ESS is mainly surgery, including an abdominal hysterectomy with bilateral salpingo-oophorectomy. Adjuvant treatment, such as radiotherapy or chemotherapy, is not routinely recommended

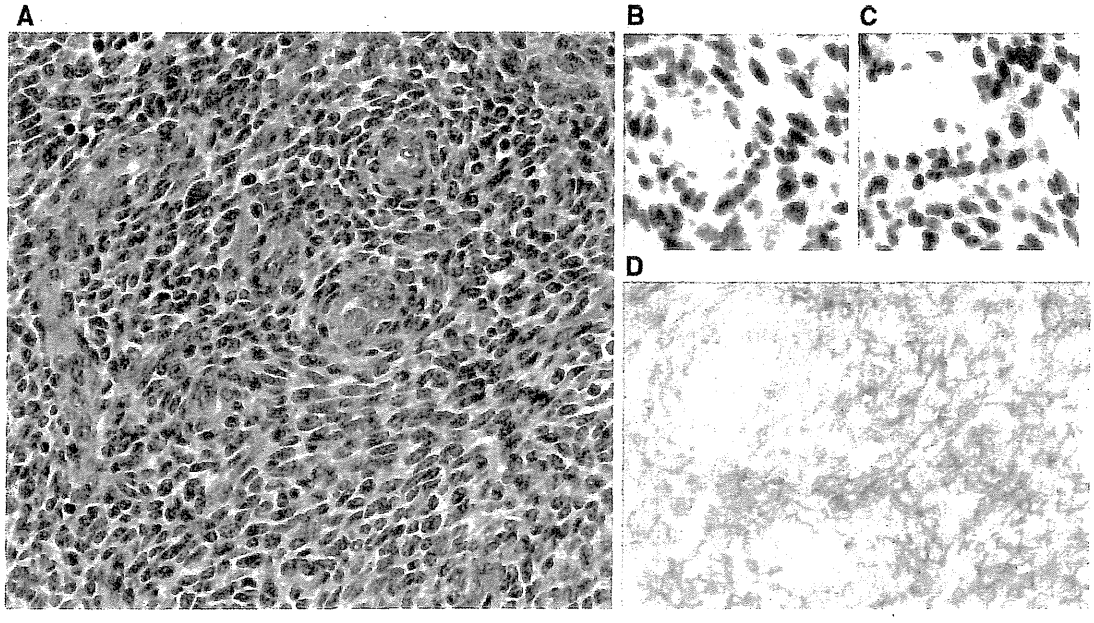

Fig. 1 Histological findings of the tumor, excised before MPA treatment. **a** High Power: Tumor cells in the pelvis, showing proliferation of endometrial stromal cells without significant atypia or pleomorphism, diagnosed as low-grade ESS. **b–d** High Power: Tumor cells are strongly positive for estrogen receptor (**b**) and progesterone receptor (**c**) and are diffusely positive for CD10 (**d**) by immunohistochemistry

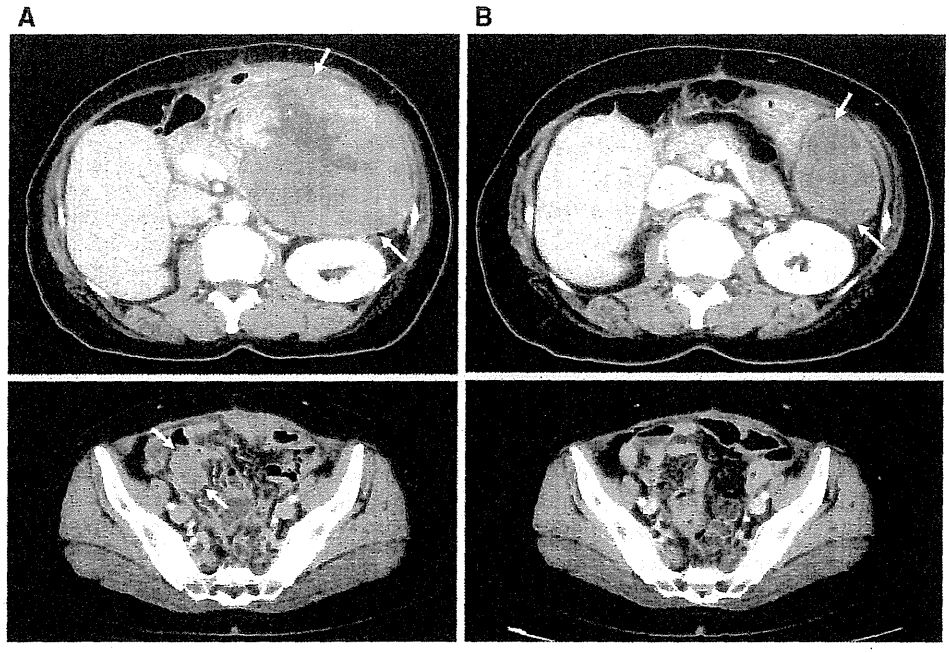

Fig. 2 Images of CT scan before and after anastrozole treatment. **a** Recurrent tumors with 13 cm in diameter in the left upper quadrant (*Upper*) and 4 cm in diameter in the pelvis (*Lower*). **b** The recurrent tumors were diminished to 7 cm in diameter (*Upper*) or became undetectable (*Lower*)

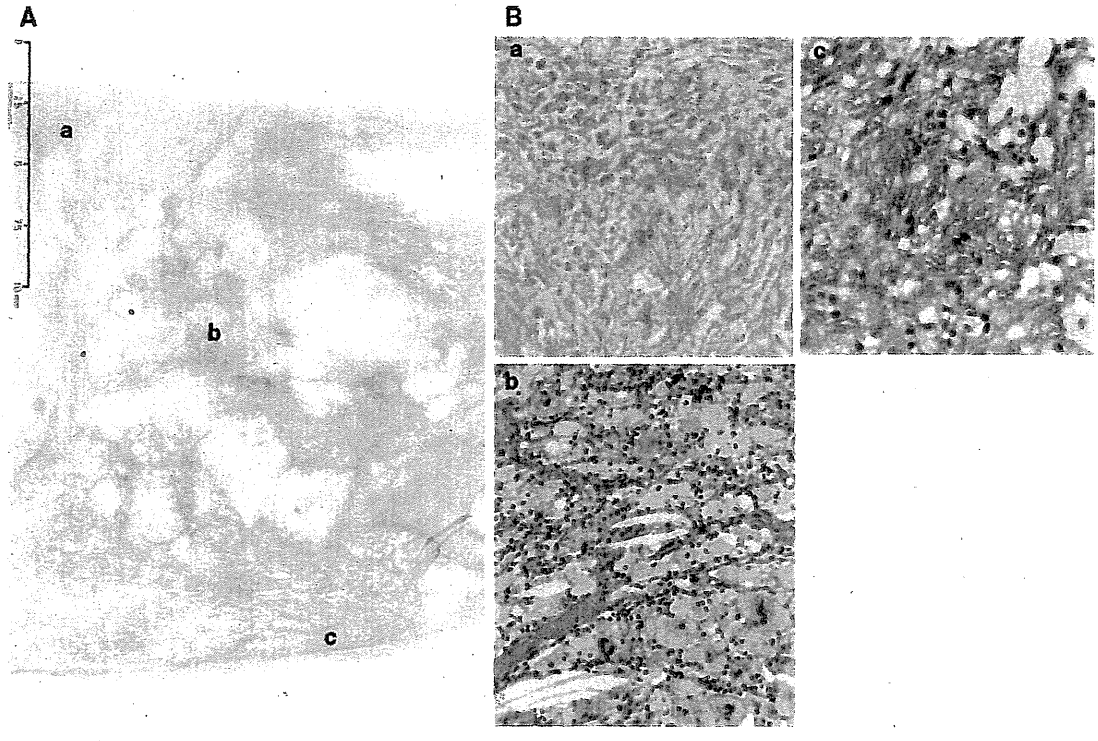

Fig. 3 Histological findings of the tumor, excised after anastrozole treatment. **a**. Low Power: Tumor cells with massive necrosis. **b** High Power: (*a*) Lesion with coagulative tumor cell necrosis, which occupies the majority of the tumor. (*b*) Center lesion with numerous foamy histiocytes. (*c*) Marginal lesion of the tumor with viable cells partly remaining

[8]. Although the prognosis of low-grade ESS is generally favorable with more than 90% of 5-year overall survival, the recurrence-free survival rate is reported to be about 50% [9, 10]. In addition to surgical resection, treatment option to recurrent low-grade ESS is hormonal therapy with progesterone derivative or aromatase inhibitor. MPA and megestrole acetate are synthetic derivatives of progesterone that exert an anti-estrogenic effect after binding to PR. The sensitivity to these progestin therapies is associated with the presence of ER and PR [11]. Aromatase inhibitors reduce estrogen levels by inhibiting its synthesis in peripheral sites. The distinct function suggests that suppressing aromatase might be still effective to recurrent ESS with resistance to progestin therapy.

The patient reported here suffered from repeated recurrences after becoming refractory to MPA treatment. Positive PR expression of the recurrent tumors suggests that the resistance to MPA therapy is caused by PR-independent manner. As a second-line hormonal therapy, anastrozole showed significant response to these recurrent tumors, suggesting that aromatase inhibitor might be useful for progestin-resistant low-grade ESS tumors. It is to be elucidated whether aromatase inhibitor is also effective to recurrent ESS tumors with negative PR expression.

Acknowledgments Conflict of interest statement All the authors declare no conflict of interest.

References

1. Koss LG, Spiro RH, Brunschwig A. Endometrial stromal sarcoma. Surg Gynecol Obstet. 1965;121:531–7.
2. Sabini G, Chumas JC, Mann WJ. Steroid hormone receptors in endometrial stromal sarcomas. A biochemical and immunohistochemical study. Am J Clin Pathol. 1992;97:381–6.
3. Wade K, Quinn MA, Hammond I, Williams K, Cauchi M. Uterine sarcoma: steroid receptors and response to hormonal therapy. Gynecol Oncol. 1990;39:364–7.
4. Gloor E, Schnyder P, Cikes M, Hofstetter J, Cordey R, Burnier F, et al. Endolymphatic stromal myosis. Surgical and hormonal treatment of extensive abdominal recurrence 20 years after hysterectomy. Cancer. 1982;50:1888–93.
5. Tsukamoto N, Kamura T, Matsukuma K, Imachi M, Uchino H, Saito T, et al. Endolymphatic stromal myosis: a case with positive estrogen and progesterone receptors and good response to progestins. Gynecol Oncol. 1985;20:120–8.
6. Maluf FC, Sabbatini P, Schwartz L, Xia J, Aghajanian C. Endometrial stromal sarcoma: objective response to letrozole. Gynecol Oncol. 2001;82:384–8.
7. Leunen M, Breugelmans M, De Sutter P, Bourgain C, Amy JJ. Low-grade endometrial stromal sarcoma treated with the aromatase inhibitor letrozole. Gynecol Oncol. 2004;95:769–71.
8. Reich O, Regauer S. Hormonal therapy of endometrial stromal sarcoma. Curr Opin Oncol. 2007;19:347–52.
9. Pink D, Lindner T, Mrozek A, Kretzschmar A, Thuss Patience PC, Dorken B, et al. Harm or benefit of hormonal treatment in metastatic low-grade endometrial stromal sarcoma: single center experience with 10 cases and review of the literature. Gynecol Oncol. 2006;101:464–9.
10. Kim WY, Lee JW, Choi CH, Kang H, Kim TJ, Kim BG, et al. Low-grade endometrial stromal sarcoma: a single center's experience with 22 cases. Int J Gynecol Cancer. 2008;18:1084–9.
11. Katz L, Merino MJ, Sakamoto H, Schwartz PE. Endometrial stromal sarcoma: a clinicopathologic study of 11 cases with determination of estrogen and progestin receptor levels in three tumors. Gynecol Oncol. 1987;26:87–97.

Cancer Science
The official journal of the Japanese Cancer Association JCA

Novel human papillomavirus type 18 replicon and its application in screening the antiviral effects of cytokines

Ayano Satsuka,[1,2] Satoshi Yoshida,[1,3] Naoko Kajitani,[1,2] Hiroyasu Nakamura[1,3] and Hiroyuki Sakai[1,4]

[1]Laboratory of Gene Analysis, Department of Viral Oncology, Institute for Virus Research; [2]Laboratory of Mammalian Molecular Biology, Graduate School of Bioscience; [3]Department of Viral Oncology, Graduate School of Medical Sciences, Kyoto University, Kyoto, Japan

(Received June 29, 2009/Revised October 9, 2009/Accepted October 19, 2008/Online publication November 16, 2009)

Human papillomaviruses (HPVs) infect the stratified epithelial organ. The infection induces benign tumors, which occasionally progress into malignant tumors. To elucidate the virus-induced tumorigenesis, an understanding of the lifecycle of HPV is crucial. In this report, we developed a new system for the analysis of the HPV lifecycle. The new system consists of a novel HPV replicon and an organotypic "raft" culture, by which the HPV-DNA is maintained stably in normal human keratinocytes for a long period and the viral vegetative replication is reproduced. This system will benefit biochemical and genetic studies on the lifecycle of HPV and tumorigenesis. This system is also valuable in screening for antiviral compounds. We confirmed its usefulness by evaluating the antivirus effect of cytokines. (*Cancer Sci* 2010; 101: 536–542)

The infection of high-risk type human papillomavirus (HPV) is a major risk factor for cervical cancer.[1–3] The World Health Organization has reported that the cases of HPV-associated cancers number about half a million, which corresponds to 10% of cancer cases in women.[4] This indicates the importance of the prevention of and urgently developing treatment for the cancer.

In order to control cervical cancer, it is essential to understand the regulatory mechanisms of the HPV infection. The primary target for HPV infection is the epithelial cells (keratinocytes) of the stratified squamous epithelium, and replication of HPV is strictly regulated by the differentiation program of the keratinocytes,[5] making it difficult to analyze the virus lifecycle in standard tissue culture systems. Several tissue culture conditions have been used for studying the differentiation-dependent lifecycle, such as a suspension culture of keratinocytes using methylcellulose "semisolid" medium,[6,7] a calcium-induced differentiation of keratinocytes,[8] and an organotypic raft culture.[9–11] Among them, the raft culture seems superior for studying the HPV lifecycle, because it is able to reproduce the stratified structure of epithelium, support the production of progeny virions in the differentiated layer, and capture the virus-induced hyperplasia as in the infected lesions. Although the raft culture has been successfully used for the analysis of the HPV lifecycle in combination with the genomic-type of HPV-DNA,[12] the drawbacks to using the culture system are the intricateness in the construction of it and the difficulty in obtaining the cell population maintaining the HPV-DNA.

In this manuscript, we tried to improve the suitability of the culture system for analysis of the HPV lifecycle. We constructed a new HPV replicon that could be maintained for a long period in comparison with the conventional method utilizing the genomic-type HPV-DNA. The raft culture system incorporating the new replicon could reproduce the physiological status of HPV-infected lesions: virus-induced hyperplasia accompanied by viral DNA amplification and late gene expression. This new system might accelerate the investigation of the HPV lifecycle. The usefulness of the system was verified by examining the effects of several cytokines on HPV replication and hyperplasia induction.

Materials and Methods

Construction of plasmid DNAs. HPV18 genomic DNA was isolated from a plasmid containing a full-length HPV18 DNA (GenBank accession no.: X05015). A new HPV18 replicon, p18FLneo, was constructed as illustrated in Figure 1. pEGFP1-ori(pBR) was constructed by replacing the origin of pEGFP1 (Clontech Laboratories, Mountain View, CA, USA) with pBR322-ori derived from pPUR (Clontech Laboratories). The long control region (LCR) of HPV18 (nucleotide number 7000 to 100; GenBank no.: X05015) was isolated by PCR, and then cloned into the vector pEGFP1-ori(pBR); the resultant plasmid was named 18LCR/pEGFP1-ori(pBR). Full-length HPV18 genome was cloned into the 18LCR/pEGFP1-ori(pBR) by using the *Afl*II recognition site. The genomic-type of HPV18 DNA was obtained by self-ligation of the full-length HPV18 DNA by following a method previously described.[13]

Cell culture and transfection. Human foreskin fibroblasts (HFFs) and human foreskin keratinocytes (HFKs) were commercially obtained (Kurabo Industries, Osaka, Japan), and maintained with 10% fetal bovine serum/DMEM and a serum-free keratinocyte growth medium (KGM) (EpiLife-KG2; Kurabo Industries), respectively. HFKs were transfected with 2 μg of p18FLneo or 1.5 μg of the genomic-type HPV18 DNA plus 0.5 μg of pEGFP1 by the nucleofection method (Nucleofector Kit; Amaxa, Cologne, Germany). The HFKs transfected with p18FLneo were cultured under the presence of G418 for more than 4 weeks, then used for the experiments.

Southern hybridization. Total DNA was extracted from the HFKs by following a standard protocol.[14] Five μg of the total DNA was digested with *Dpn*I and *Bgl*I, and then the DNA fragments were separated by 0.8% agarose gel electrophoresis, and transferred to a nylon membrane (Hybond N+; Amersham Biosciences UK, Little Chalfont, UK). For the detection of HPV18-specific DNA, a non-RI detection system was employed (Digoxigenin [DIG] Wash and Block Buffer Set and anti-DIG-alkaline phosphatase [AP]; Roche Diagnostics, Mannheim, Germany). The DIG-labeled probe for the LCR (7000–100 nt; GenBank no.: X05015) or L1 region (6137–7136 nt; GenBank no.: X05015) of HPV18 was obtained by a PCR-mediated method (PCR DIG Probe Synthesis Kit; Roche Applied Science, Manheim, Germany). The chemiluminescent signal

[4]To whom correspondence should be addressed.
E-mail: hsakai@virus.kyoto-u.ac.jp

doi: 10.1111/j.1349-7006.2009.01411.x

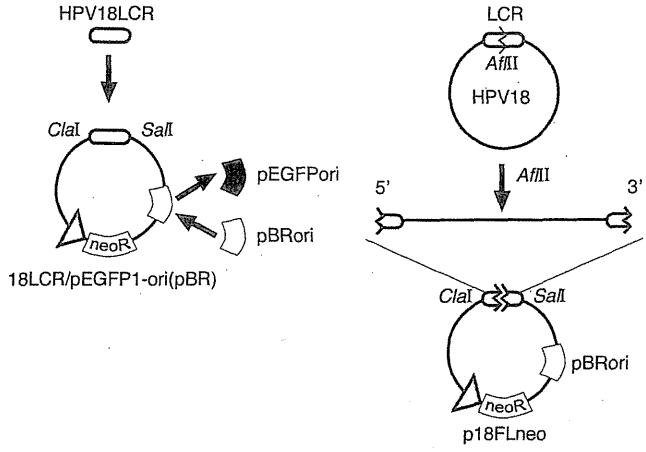

Fig. 1. Structure of a new human papillomavirus (HPV) replicon. A new replicon containing the full length of HPV18 genomic DNA constructed with a backbone plasmid, pEGFP1-ori(pBR), based on pEGFP1 plasmid. The replication origin (ori) element was replaced with that of pBR322. HPV18 long control region (LCR) was cloned into the pEGFP1-ori(pBR), and then the full-length HPV18 genome was inserted into the AflII site located in the LCR region. The obtained replicon was named p18FLneo.

was visualized with a chemiluminescent image analyzer (LAS-3000; Fuji Film, Tokyo, Japan).

Organotypic raft culture system. The construction of the organotypic raft culture and the preparation of frozen section have been described previously.[15–17] For BrdU incorporation, 50 g/mL BrdU (Sigma-Aldrich, St Louis, MO, USA) was added in the medium 6 h before harvest. The thickness of the epidermal layer was measured using image analysis software (AxioVision 3.1; Carl Zeiss Vision, Munich, Germany).

Immunoblot analysis. Total cell lysate of HFKs was obtained with a triple-detergent buffer (50 mM Tris-HCl [pH 8.0], 150 mM NaCl, 0.02% sodium azide, 0.1% sodium dodecyl sulfate [SDS], 1% Nonidet P-40, 0.5% sodium deoxycholate)[18] supplemented with a protease inhibitor cocktail (0.5 mM PMSF, 0.15 M aprotinin, 1 M E-64, 1 M leupeptin, 0.5 M EDTA) (Nakarai Tesuque, Kyoto, Japan) and 1 mM dithiothreitol. Equal amounts of cell lysate (5 μg protein) were subjected to SDS–polyacrylamide gel electrophoresis (SDS-PAGE) and the gel was blotted to a PVDF membrane (Hypond-P; Amersham Biosciences UK). The equalities of the loaded amounts were confirmed with the anti-actin immunoblot (1:50000) (clone AC-15; Sigma-Aldrich) (data not shown). Antibodies for p53 (1:1000) (Ab-6; Oncogene Research Products, San Diego, CA, USA) and pRb (1:1000; BD Biosciences Pharmingen, San Diego, CA, USA) were purchased commercially. Horseradish peroxidase (HRP)-conjugated secondary antibodies (1:3000; Amersham Biosciences UK) and a luminal reagent (Western Blotting Luminol Reagent; Santa Cruz Biotechnology, Santa Cruz, CA, USA) were purchased commercially. The chemiluminescent signal was visualized with a chemiluminescent image analyzer (LAS-3000; Fuji Film).

Immunohistochemistry (IHC). IHC for the tissue sections on slide glasses was performed as described previously.[15–17] Antibodies for BrdU (1:400) (clone 2B-1; MBL, Nagoya, Japan) and L1 (1:200) (MAB837; Millipore, Billerica, MA, USA), and p53 (Ab-6) (Oncogene Research Products), and pRb (BD Biosciences Pharmingen) were purchased commercially.

***In situ* hybridization (ISH).** Detection of HPV18 DNA signals in the tissue sections was performed with the TSA-biotin system (Perkin-Elmer, Boston, MA, USA) following the manufacturer's instructions. The DIG-labeled DNA for HPV18 LCR region (7000–100 nt; GenBank no.: X05015) (DIG high prime; Roche Diagnostics) was used as the probe. For the detection of DIG-labeled probe, HRP-labeled anti-DIG antibody (Dako, Glostrup, Denmark) was used. After hybridization, biotinyl tyramide working solution, SA-HRP (streptavidin–HRP), and metal-enhanced DAB solution (Roche Diagnostics) was used for detection of the signal. All slides were counterstained with hematoxylin.

Cytokine treatment. In monolayer culture, HFKs were incubated with cytokines (interferon [IFN]-β, 100 units/mL; transforming growth factor [TGF]-β, 1 ng/mL; tumor necrosis factor [TNF]-α, 5 ng/mL) for 3 days. IFNβ and TGFβ (Sigma-Aldrich) and TNFα (Merk Biosciences, San Diego, CA, USA) were purchased from the distributors. In the organotypic raft culture, cytokines were added in the culture medium for 7 days before the sample harvest.

Apoptosis induction by cytokine. 2×10^5 cells were cultured in the growth medium supplemented with the cytokines for 3 days. The treated cells were washed, trypsinized, and fixed with ice-cold methanol. Apoptotic cells were labeled by M30 antibody (CytoDEATH; Roche Diagnostics) and AlexaFLUOR488-antimouse antibody (Invitrogen, Carlsbad, CA, USA), and then counted by flow cytometry (BD Biosciences, San Jose, CA, USA).

Results

Construction of new HPV replicon. Genomic-type HPV-DNA was used as the replicon to obtain the keratinocytes maintaining HPV-DNA. The genomic-type DNA, which was constructed by re-circularization of full-length HPV-DNA, was transfected into the cells with the pSV2*neo* expressing a neomycin-resistance gene (neo^R).[13] The transfected cells were selected in the culture medium containing G418 for about 1 week, and then the surviving cells were expanded without the drug selection. The raft culture constructed with the cells could reproduce viral vegetative replication as reported previously.[12] By this method, there is no selectable pressure for the maintenance of HPV-DNA, causing a possible problem in that the cells lose HPV-DNA. It was also suggested that the transfection of the genomic-type DNA was inefficient because of its non-supercoiled structure.[19] To eliminate this potential problem, full-length HPV18 DNA was inserted into a plasmid containing the neo^R expression unit (Fig. 1). The replication of HPVs is regulated by the LCR as the promoter/enhancer for gene expressions at the 5′ region of the coding region and as the transcriptional terminator at the 3′ region. Therefore, the LCR was added at the both sides of the coding region. We named the new replicon p18FLneo (FL is an abbreviation for full length).

We verified the potential of p18FLneo as the replicon by examining whether it could be maintained stably in culture cells. HFKs were transfected with p18FLneo, then cultured under the presence of G418 for 4 weeks. Under the same condition, we found that the mock-transfected cells were dislodged within a week and that the cells transfected with pEGFP1, which contains the neo^R expression unit and is replication-defective in the HFKs, could not survive for more than 2 weeks. The total DNAs were collected from the cells, and then HPV-DNA was detected by Southern hybridization analysis. The result indicated that p18FLneo was stably maintained in the HFKs as a HPV18 replicon (Fig. 2A, p18FLneo). In order to validate its potential as the replicon, the genomic-type of HPV18 DNA was used as the control replicon (Fig. 2A, 18-ligation). The genomic-type HPV18 was introduced with the pEGFP1 into the HFKs. The transfected cells were selected under the presence of G418 for 1 week, and then the surviving cells were cultured without the drug-selection for 3 weeks. The amount of replicated HPV-DNA was analyzed by Southern blot analysis, and it appeared that the efficiency of the maintenance or the replication of the genomic-type HPV18

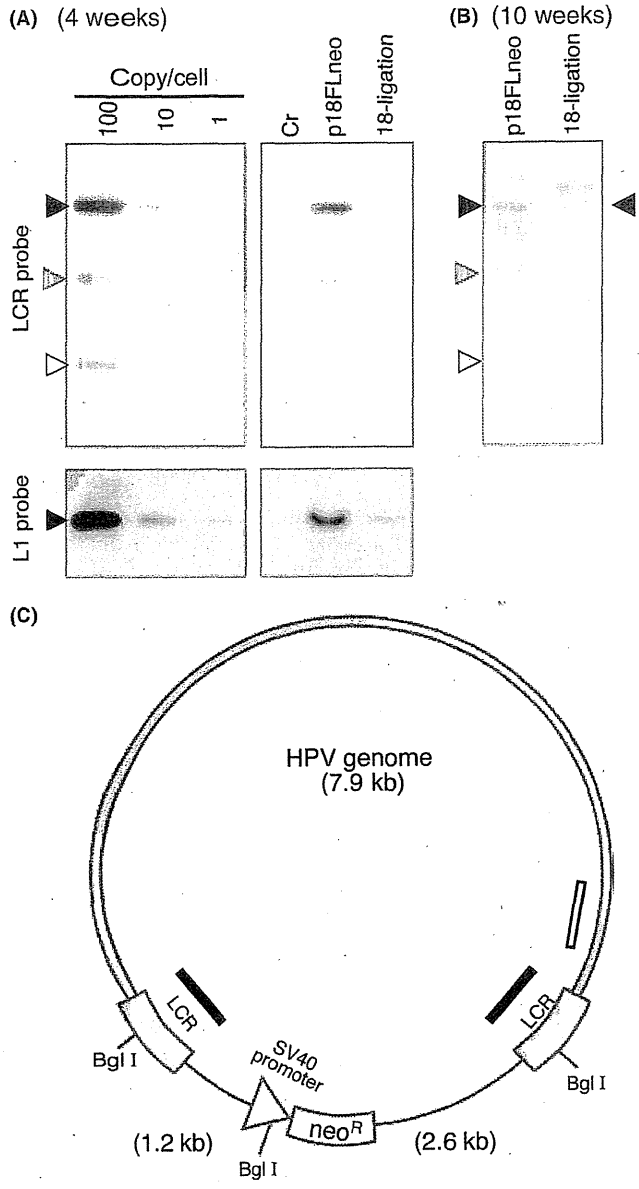

Fig. 2. Maintenance of the new human papillomavirus (HPV) replicon in primary keratinocytes. (A) Maintenance of the HPV replicon in the human foreskin keratinocytes (HFKs) 4 weeks after transfection was examined by Southern blot analysis. Total DNA was extracted from the normal HFKs (Cr), the HFKs harboring either the HPV replicon (p18FLneo) or the genomic-type HPV18 DNA (18-ligation) and subjected to *Dpn*I + *Bgl*I digestion. Each lane was loaded with 5 μg of the total DNA. p18FLneo DNA was used as the control for the copy number per cell. p18FLneo was digested with *Bgl*I and applied to the agarose gel at an amount equivalent to 1 copy, 10 copies, or 100 copies per cell. The probe used for the detection of HPV-DNA was DIG-labeled 18LCR or 18L1 DNA fragment. Closed triangle indicates the position of the full-length HPV18 genomic DNA. Gray and open triangles indicate the positions of the fragments containing a portion of long control region (LCR) and the backbone plasmid; those fragments could not be detected with L1 probe. (B) The maintenance of the HPV replicon in HFKs 10 weeks after transfection was examined as described in (A). Closed triangle indicates the position of the full-length HPV18 genomic DNA. Gray and open triangles indicate the positions of the fragments containing a portion of LCR and the backbone plasmid. The extra signals observed in each lane were considered the integrated form of HPV-DNA. (C) The scheme of pFL18neo. Gray region indicates HPV18 DNA. Black and white bars indicate the regions targeted by LCR and L1 probes, respectively. The recognition sites for BglI are indicated, and the digestion produced three DNA fragments, 7.9 kb, 2.6 kb, and 1.2 kb.

DNA was lower than that of p18FLneo. These results suggested the advantage of p18FLneo as the HPV replicon.

The HFKs containing p18FLneo could be maintained for more than 10 weeks under the presence of G418. The growth potential of normal HFKs apparently declined after 6 weeks of culturing and the cells acquired senescence status, indicating that the HFKs containing p18FLneo were immortalized by the functions of HPV E6 and E7. The existence of HPV-DNA in the cells was examined, and it was revealed that the majority of HPV-DNA was maintained as the episomal status and that some portion of the DNA might be integrated in the host chromosome (Fig. 2B, p18FLneo). In the accompanying experiment, the DNA status in the HFKs containing the genomic-type HPV-DNA was examined, and it found that most of the HPV-DNA was maintained as integrated form (Fig. 2B, 18-ligation).

Raft culture with HFKs harboring the new HPV replicon. The HFKs or the spontaneously immortalized keratinocytes (normal immortal keratinocytes, NIKS)[20] harboring HPV genomic DNA were used to organize the organotypic raft culture,[11,13,21,22] and they could support HPV replication in a differentiation-dependent manner. We examined whether the HFKs maintaining p18FLneo ($HFK_{p18FLneo}$) could also support the HPV lifecycle in the raft culture.

$HFK_{p18FLneo}$ could organize a stratified epithelial structure and it appeared that significant hyperplasia was induced (Fig. 3, H&E). In the epithelial layer of the $HFK_{p18FLneo}$ raft culture, BrdU-positive cells were detected in the parabasal layer. On the contrary, BrdU-positive cells were restricted at the basal layer in the raft culture with normal HFKs (Fig. 3, BrdU). This observation suggested that p18FLneo had the potential to disturbe the differentiation program of the epithelial cells and induced hyperproliferation.

We next examined whether the late-phase of the virus lifecycle was reproduced with $HFK_{p18FLneo}$. By ISH with the HPV18 probe, the cells positive for HPV18 DNA were detected in the suprasurface layer (Fig. 3, ISH), indicating that the copy number of p18FLneo was amplified in the differentiated layer of the epithelium. The expression of the late gene product, L1, was also detected in the differentiated layers by IHC (Fig. 3, IHC). These observations indicate that $HFK_{p18FLneo}$ in combination with the raft culture is an appropriate tool for the analysis of the HPV lifecycle. Although the $HFK_{p18FLneo}$ maintained for long period (10 weeks) was also used for the raft culture, it failed to organize a stratified epithelial layer, indicating it lost the property of normal cellular differentiation.

Application of the new HPV replicon: (1) Effects of cytokines on the latent phase of HPV infection. Cytokine production is a biological response *in vivo* to virus infection or inflammation. One of the cytokines, type I IFN, is used in chemotherapy for HPV-positive cervical neoplasia.[23] Other cytokines, TGFβ and TNFα, have been reported to be involved in the response to HPV infection.[24–30] We examined the effects of these cytokines on HPV replication using the new HPV replicon system.

The monolayer culture of $HFK_{p18FLneo}$ is supposed to represent the status of the latent infection of HPV in basal cells. We first examined the effects of the cytokines on the $HFK_{p18FLneo}$ monolayer culture. We chose doses of cytokines that had minimal effects on the growth of normal HFKs (IFNβ, 100 units/mL; TGFβ, 1 ng/mL; TNFα, 5 ng/mL) in order to observe the specific effects on HPV replication (Fig. 4). These doses of the cytokine treatments had also no significant effects on the growth of $HFK_{p18FLneo}$. The apoptosis induction by the cytokines was also examined by FACS analysis using an apoptosis-specific antibody (M30 CytoDEATH; Roche Diagnostics), and it appeared that these cytokine treatments did not induce any apoptotic response (data not shown). Note that the treatment of higher doses of the cytokines induced growth arrest or

doi: 10.1111/j.1349-7006.2009.01411.x

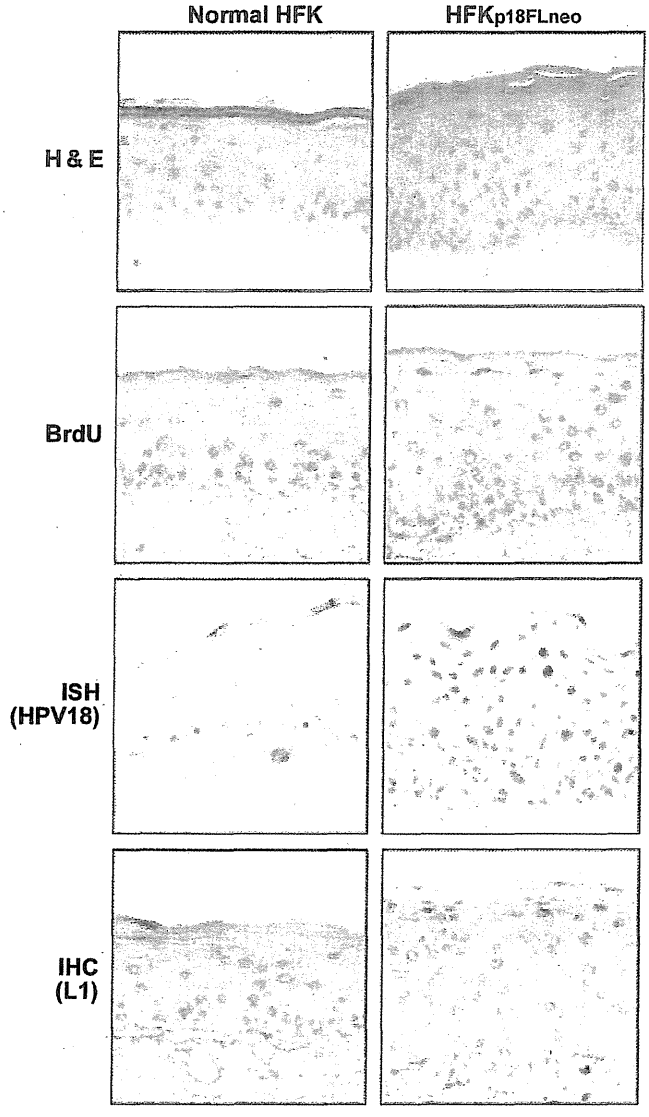

Fig. 3. Vegetative replication of the human papillomavirus (HPV) replicon in the raft culture. Thin sections (7 μm) were obtained from the raft culture organized with normal human foreskin keratinocytes (HFKs) and $HFK_{p18FLneo}$. The DNA synthesis of the cell was monitored by immunohistochemistry for incorporated BrdU. HPV18 DNA was detected by *in situ* hybridization (ISH) with DIG-labeled L1 probe. The expression of L1 protein was analyzed by IHC with anti-L1 antibody.

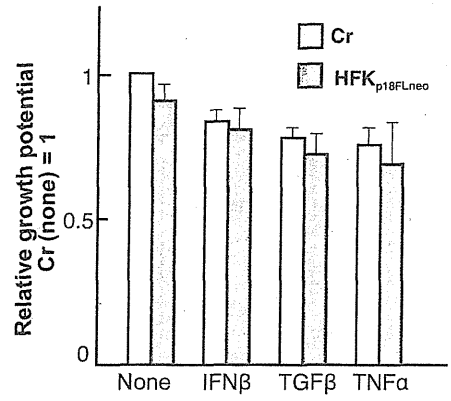

Fig. 4. Effects of cytokines on the proliferation of human foreskin keratinocytes (HFKs) harboring p18FLneo. The effects of cytokine treatments (interferon [IFN]-β, 100 units/mL; transforming growth factor [TGF]-β, 1 ng/mL; tumor necrosis factor [TNF]-α, 5 ng/mL) on the proliferation of HFKs were monitored. The growth rate in 72-h culture of the exponentially growing cells is indicated (growth rate of not treated normal HFKs, 1). The living cells were distinguished by Trypan blue exclusion. The value is the average of at least three independent experiments and the SD is indicated.

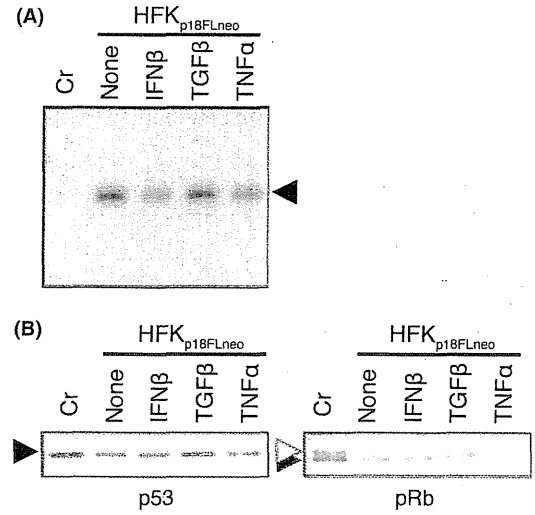

Fig. 5. Effects of cytokines on the maintenance of the human papillomavirus (HPV) replicon. (A) The $HFK_{p18FLneo}$ was treated with cytokines for 3 days and total DNA was extracted. The DNA was digested with both BglI and DpnI and 2 μg of it was subjected to Southern blot analysis with the DIG-labeled L1 probe. Normal human foreskin keratinocytes (HFKs) were used as the control (Cr). (B) Expressions of p53 and pRb in the same cells monitored by immunoblot analysis.

apoptotic cell death of both normal HFKs and $HFK_{p18FLneo}$ (data not shown).

Next, we examined the effects of the cytokines on the maintenance of HPV-DNA in $HFK_{p18FLneo}$, and the result indicated that IFNβ treatment moderately suppressed HPV-DNA replication (Fig. 5A). The TGFβ and TNFα treatments did not influence DNA maintenance significantly. In HPV-infected cells, the expressions of cellular tumor suppressors p53 and pRb are suppressed by the functions of viral oncoproteins E6 and E7, respectively. We analyzed the expressions of p53 and pRb in $HFK_{p18FLneo}$ by immunoblot analysis, and found that they slightly decreased as compared with those in the normal HFKs (Fig. 5B). This weak suppression indicated that the expression levels of the viral oncoproteins were kept low as found in the latent infection of HPV. The weak suppressions of p53 and pRb expressions were not modified significantly by the cytokine treatments.

The results indicated that the cytokine treatments used in this report did not affect the growth potential of $HFK_{p18FLneo}$ and the maintenance of HPV-DNA. Given that $HFK_{p18FLneo}$ is considered to represent basal cells latently infected with HPV, these results suggested that the cytokine treatments had no anti-HPV effect on the latently infected cells.

Application of the new HPV replicon: (2) Effects of cytokines on the late-stage of the HPV lifecycle. We next examined the effect of the same set of cytokines on the late-stage of the HPV lifecycle by using $HFK_{p18FLneo}$ and the raft culture. As described above, the raft culture with $HFK_{p18FLneo}$ showed a moderate hyperplasia at the epithelial layer (Fig. 3), and the hyperplasia

could be suppressed by the IFNβ treatment to the level of normal HFKs (Fig. 6). The number of BrdU-positive cells in the upper layers of epithelium was decreased with IFNβ treatment (Fig. 7, BrdU). As compared with IFNβ, the moderate but significant suppression could be also observed with TGFβ. In contrast, the TNFα could not suppress hyperplasia formation and it activated the invasive potential of the epithelial cells. The number of BrdU-positive cells was rather increased with TNFα. These results indicated that IFNβ treatment had an apparent suppressive effect on virus-induced hyperplasia. The results also raised the possibility that TNFα treatment accelerated virus-induced tumorigenesis.

Next, the effect of the cytokine treatment on the vegetative viral replication was analyzed. The amplification of viral DNA at the upper layer of epithelium was suppressed by the treatment of IFNβ and TGFβ (Fig. 7, ISH). On the other hand, TNFα treatment activated viral DNA amplification in the broad area of the epithelium. These observations indicated that both IFNβ and TGFβ could suppress the late phase in the HPV lifecycle and TNFα treatment had the opposite effect on it.

It is considered that the viral oncoproteins E6 and E7 are responsible for virus-induced hyperplasia.[31] We examined the effects of cytokines on the status of p53 and pRb in the raft culture in order to estimate the expression levels of E6 and E7, respectively. The expressions of p53 and pRb were decreased in the epithelial layer of the $HFK_{p18FLneo}$ raft culture as compared to those of normal HFKs (Fig. 7, p53 and pRb). It was supposed that this decrement was caused by the E6 and E7 expressed moderately in $HFK_{p18FLneo}$. IFNβ treatment recovered p53 expression at the middle layers of epithelium, although TGFβ did not modify the p53 status. TNFα enhanced p53 expression in the epithelium broadly. pRb expression was slightly recovered by all three cytokine treatments. These results indicated that the cytokines affected the expressions of p53 and pRb, although their relation to the antiviral effect remains unclear.

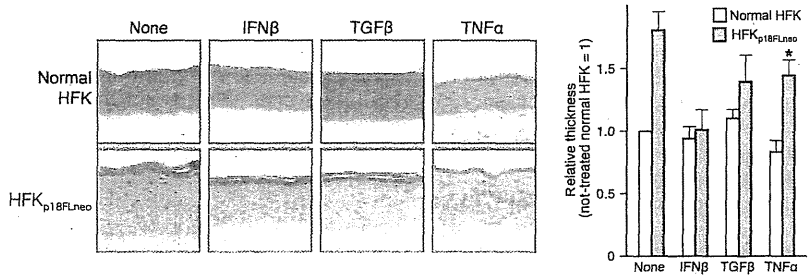

Fig. 6. Effects of cytokines on the raft culture constructed with human foreskin keratinocyte $(HFK)_{p18FLneo}$. Effects of cytokine treatments on the raft culture organized with normal HFKs or $HFK_{p18FLneo}$ were examined. Frozen-sections of the raft culture were fixed with 4% paraformaldehyde and stained with H&E. The thickness of the epidermis was estimated by microscopic analysis with an image analysis application (AxioVision; Carl Zeiss Vision), and the relative values are indicated as a bar chart (thickness of not treated normal HFK set as 1.0; average value, 95 μm). The value is the average of at least three independent experiments and the SD is indicated. Note that the epidermis of the $HFK_{p18FLneo}$ treated with tumor necrosis factor (TNF)-α exhibited the invasion phenotype; therefore, the thickness of it could not be measured precisely (indicated with an asterisk).

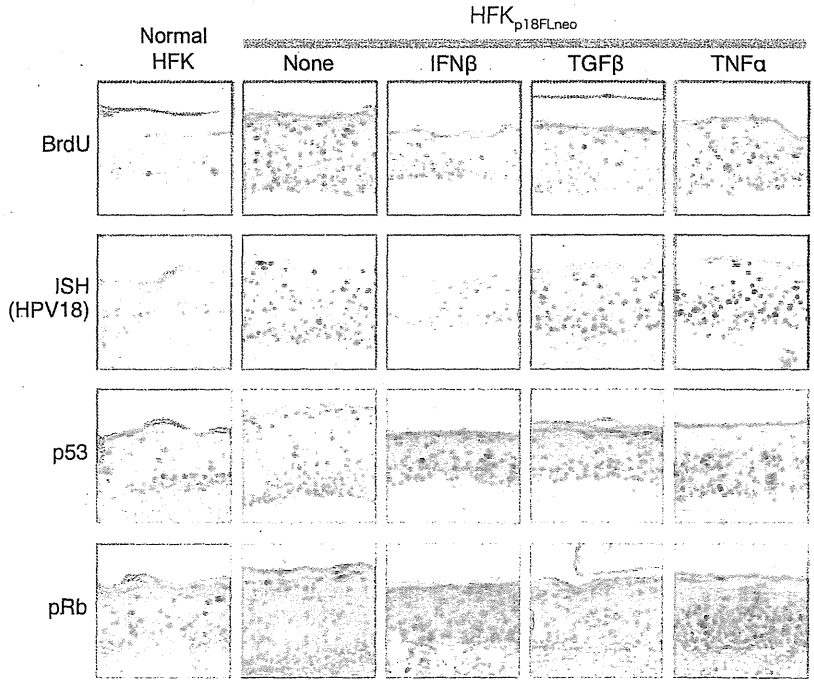

Fig. 7. The effects of cytokine treatments on human papillomavirus (HPV) replication. Effects of cytokine treatments on HPV replication and on cellular status were examined by using the raft culture. The DNA synthesis of the cells was monitored by the uptake of BrdU. Incorporated BrdU was detected by immunohistochemistry (IHC) with anti-BrdU antibody. HPV-DNA was detected by *in situ* hybridization (ISH) with DIG-labeled 18L1 probe (ISH). The expressions of p53 and pRb in the raft culture were monitored by IHC with specific antibodies (p53 & pRb).

doi: 10.1111/j.1349-7006.2009.01411.x

Discussion

A novel HPV replicon. We constructed a new replicon of HPV by integrating several improvements for the stable maintenance of the replicon in the cells, which made it easy to collect cells harboring HPV-DNA. The major points are summarized below.

- The HPV replicon has a configuration of plasmid DNA, not of genomic DNA. In previous reports, the genomic-type of DNA was used as a replicon. To obtain the genomic-structure of DNA, full-length HPV-DNA was excised from a plasmid and circularized by self-ligation.[13] This process is laborious and it is difficult to control the quality of the DNA, which influences the transfection efficiency. The self-ligated DNA has a non-supercoiled configuration, and such a form of DNA might not be an appropriate substrate for gene expression and DNA replication. We incorporated, therefore, the HPV-DNA into a plasmid backbone, which made it easier to control the DNA quality and the constancy of the transfection efficiency was improved.
- In the conventional protocol for obtaining the HFKs harboring HPV-DNA, HFKs were transfected with both the genomic-type of DNA and a plasmid expressing a drug-resistance gene, such as pSV2*neo*.[13] After a short period of drug selection, the cells were then expanded without drug selection. The HPV replicon used in this report contained a selection marker, an expression unit for a neomycin-resistance gene, which made it possible to apply the drug-selection even in the expansion process, ensuring that the obtained cells maintained HPV replicons.

In addition to these points, it is unique that p18FLneo contains the LCR at both sides of the genome (Fig. 1). Although we designed it by taking into account the roles of the LCR as 5′- and 3′-regulatory elements, the artificial structure might have unexpected effects on HPV replication. It is necessary, therefore, to compare carefully the replication potentials between the genomic-type DNA and p18FLneo. We also need to determine whether the 3′-LCR unit is required for the maintenance or vegetative replication of HPV-DNA.

Recently Wang *et al.* reported a new system for analyzing the HPV18 lifecycle.[19] They used a plasmid containing HPV18 genome into which a neo^R expression unit and loxP sites were inserted. The plasmid was co-transfected into human keratinocytes along with an expression plasmid for a Nuclear Localization Signal (NLS)-tagged Cre recombinase, resulting in efficient establishment of the cells maintaining almost authentic HPV18 genomic DNA. The most important improvement seemed that they used plasmid DNA instead of the self-ligated genomic-type DNA that did not have a supercoiled structure. The system described in this paper employed a plasmid DNA, p18FLneo, as a replicon, suggesting it has the similar advantage. The long-term selection under the G418 presence is able to be adapted in the system with p18FLneo, but not in the system reported by Wang *et al.* Although their system could produce very high titer of infectious virus, what made this improvement was unexplained, as commented in a review.[32] It will be necessary to perform side-by-side comparison between the systems using p18FLneo and the plasmids used by Wang *et al.*

Usefulness of the new system supporting efficient HPV replication. The new HPV replicon could be maintained stably in HFKs as shown in Figure 2. When applied in the raft culture, the HFKs maintaining the replicon showed moderate hyperplasia and the HPV-DNA was amplified at the differentiated layer of epidermis (Fig. 3). The hyperplasia observed with the raft culture was moderate as compared with that induced by high-risk type E7 expression.[16] The immunoblot analysis of p53 and pRb expressions in the HFKs indicated that the introduction of the HPV replicon suppressed moderately those expressions, suggesting the E6 and E7 expression levels in the HFKs were maintained at low level. It is supposed that the expressions of E6 and E7 are up-regulated in the course of malignant conversion of the HPV-infected cells,[33] thus, the raft culture harboring the HPV replicon seems to represent an early stage of the tumor induced by the HPV infection.

Effects of cytokines in protection against virus infection. Living organisms have protection systems for the viral infections. In mammals, a variety of cytokines are produced by either infected cells or periphery cells, which act in the elimination of the infected cells.[34] The system using the new HPV replicon and the raft culture could be used to examine the effect of cytokine treatment on the early stage of HPV-infected lesions. We selected three cytokines, IFNβ, TNFα, and TGFβ, because there were several reports indicating the relation between these cytokines and HPV infection.[24–30,35,36]

We first examined the effects of the cytokines on the monolayer culture of the HFKs harboring the HPV replicon, which represented the status of the HPV-infected basal cells. Under this condition, although IFNβ treatment could suppress HPV-DNA replication moderately, the treatments of other cytokines, TGFβ and TNFα, had almost no effect on both HPV-DNA replication and cell proliferation (Figs 4,5). HFKs harboring the 18FLneo under the monolayer culture condition showed little signature of viral infection, and the cytokine treatments examined here might not display their effect on such cells. On the contrary, it has been reported that these cytokines have suppressive effects on the growth of HPV-positive cell lines.[24–27,35,36] The cells used in those reports have malignant or transformed phenotype, which might have cause observations different from ours.

Next, the effects were examined using the raft culture (Fig. 6). Under this condition, IFNβ exhibited strong inhibitory effects on dysplasia formation. It also suppressed the vegetative replication of the virus in the suprabasal layer of epithelium. TGFβ also exhibited a significant inhibitory effect on both dysplasia formation and HPV-DNA amplification, but the effect was not as drastic as that of IFNβ. In contrast, it appeared that TNFα treatment enhanced HPV replication and induced the invasion of epithelial cells into the dermal layer.

IFNβ has been administered to HPV-infected lesions including condylomas and early stage cervical intraepithelial neoplasia [23] By using this model, it was possible to confirm the effectiveness of IFNβ on the treatment of HPV-related lesions under tissue culture condition, indicating that this system is a useful platform for examination of the detailed action-mechanisms of IFNβ on HPV replication. Recently, it was reported that p56, a product of ISG56, interacted with viral replication factor E1 and inhibited its function.[37] It will be interesting to examine the induction level of p56 by IFNβ treatment in both the monolayer and raft cultures.

It should be noted that the expressions of E6 and E7 are usually up-regulated in the advanced stages of cervical neoplasia, and they were reported to interfere with the IFN-related pathway by interacting with Tyk2,[38] IRF3,[39] IRF1,[40] or IRF9.[41] Although this report described the significant anti-HPV effects of IFNβ, such effects might be diminished in association with the progression of malignant status.

The observation that TNFα treatment enhanced HPV replication suggests that the inflammatory response accompanied by TNFα production exerts effects opposite to the antiviral response at the early stage of HPV-infected lesions. In searching for new therapeutic approaches to HPV-related diseases, it might be important to consider the induction of inflammation, which has the potential to accelerate disease progression.

In this report, we developed a new experimental system that could support the replication of HPV-DNA for a long period

and the differentiation-dependent lifecycle of the virus. This system will be adapted to screening for other anti-HPV compounds. It also allows the manipulation of the genetic elements of both host cells and virus; thus, the analysis of regulatory mechanisms of the virus lifecycle and virus-induced tumorigenesis becomes accessible.

Acknowledgments

We thank the many colleagues for technical assistance and manuscript preparation, K. Sasaki for essential advice and support, Dr. P.M. Howley for providing full-length clones for HPV18, and Dr. M. Tsunenaga and Dr. T. Kuroki for instructions regarding the organotypic raft culture. This work is supported in part by a Grant-in-Aid from the Ministry of Health, Labor and Welfare of Japan for the Third-Term Comprehensive 10-year Strategy for Cancer Control. A.S., S.Y., N.K., and H.N. were supported by the 21st Century COE program of the Japan Society for the Promotion of Science (JSPS).

References

1 Howley PM, Lowy DR. Papillomavirus and their replication. In: Knipe DM, Howley PM, eds. *Fields Virology*, 5th edn. Hagerstown: Lippincott Williams & Wilkins,a Wolters Kluwer Business, 2007; 2299–354.
2 Durst M, Gissmann L, Ikenberg H, Zur Hausen H. A papillomavirus DNA from a cervical carcinoma and its prevalence in cancer biopsy samples from different geographic regions. *Proc Natl Acad Sci U S A* 1983; **80**: 3812–5.
3 Zur Hausen H. Papillomavirus infections–a major cause of human cancers. *Biochim Biophys Acta* 1996; **1288**: F55–78.
4 Castellsagué X, De Sanjosé S, Aguado T *et al.* HPV and cervical cancer in the 2007 report. *Vaccine* 2007; **25** (Suppl 3): C1–230.
5 Longworth MS, Laimins LA. Pathogenesis of human papillomaviruses in differentiating epithelia. *Microbiol Mol Biol Rev* 2004; **68**: 362–72.
6 Flores ER, Lambert PF. Evidence for a switch in the mode of human papillomavirus type 16 DNA replication during the viral life cycle. *J Virol* 1997; **71**: 7167–79.
7 Adams JC, Watt FM. Fibronectin inhibits the terminal differentiation of human keratinocytes. *Nature* 1989; **340**: 307–9.
8 Ruesch MN, Laimins LA. Human papillomavirus oncoproteins alter differentiation-dependent cell cycle exit on suspension in semisolid medium. *Virol* 1998; **250**: 19–29.
9 Meyers C, Frattini MG, Hudson JB, Laimins LA. Biosynthesis of human papillomavirus from a continuous cell line upon epithelial differentiation. *Science* 1992; **257**: 971–3.
10 Dollard SC, Wilson JL, Demeter LM *et al.* Production of human papillomavirus and modulation of the infectious program in epithelial raft cultures. *OFF Genes Dev* 1992; **6**: 1131–42.
11 Frattini MG, Lim HB, Laimins LA. In vitro synthesis of oncogenic human papillomaviruses requires episomal genomes for differentiation-dependent late expression. *Proc Natl Acad Sci U S A* 1996; **93**: 3062–7.
12 Moody CA, Fradet-Turcotte A, Archambault J, Laimins LA. Human papillomaviruses activate caspases upon epithelial differentiation to induce viral genome amplification. *Proc Natl Acad Sci U S A* 2007; **104**: 19541–6.
13 Frattini MG, Lim HB, Doorbar J, Laimins LA. Induction of human papillomavirus type 18 late gene expression and genomic amplification in organotypic cultures from transfected DNA templates. *J Virol* 1997; **71**: 7068–72.
14 Strauss WM. Preparation of genomic DNA from mammalian tissue. In: Ausubel FM, Brent R, Kingston RE *et al.*, eds. *Current Protocols in Molecular Biology*. New York: John Wiley & Sons, Inc., 1998; 2.1–2.3.
15 Yoshida S, Kajitani N, Satsuka A, Nakamura H, Sakai H. Ras modifies proliferation and invasiveness of cells expressing human papillomavirus oncoproteins. *J Virol* 2008; **82**: 8820–7.
16 Ueno T, Sasaki K, Yoshida S *et al.* Molecular mechanisms of hyperplasia induction by human papillomavirus E7. *Oncogene* 2006; **25**: 4155–64.
17 Tsunenaga M, Kohno Y, Horii I *et al.* Growth and differentiation properties of normal and transformed human keratinocytes in organotypic culture. *Jpn J Cancer Res* 1994; **85**: 238–44.
18 Sambrool J, Fritsch EF, Maniatis T. *Molecular Cloning*. New York: Cold Spring Harbor Laboratory Press, 1989; 18.30–3.
19 Wang HK, Duffy AA, Broker TR, Chow LT. Robust production and passaging of infectious HPV in squamous epithelium of primary human keratinocytes. *Genes Dev* 2009; **23**: 181–94.
20 Allen-Hoffmann BL, Schlosser SJ, Ivarie CA, Sattler CA, Meisner LF, O'Connor SL. Normal growth and differentiation in a spontaneously immortalized near-diploid human keratinocyte cell line, NIKS. *J Invest Dermatol* 2000; **114**: 444–55.
21 Flores ER, Allen-Hoffmann BL, Lee D, Sattler CA, Lambert PF. Establishment of the human papillomavirus type 16 (HPV-16) life cycle in an immortalized human foreskin keratinocyte cell line. *Virol* 1999; **262**: 344–54.
22 Flores ER, Allen-Hoffmann BL, Lee D, Lambert PF. The human papillomavirus type 16 E7 oncogene is required for the productive stage of the viral life cycle. *J Virol* 2000; **74**: 6622–31.
23 Frazer IH, McMillan NAJ. Papillomatosis and condylomata acuminata. In: Penny S-HaRW, ed. *Clinical Applications of the Interferons*. London: Chapman and Hall Medical, 1997; 79–91.
24 Donalisio M, Cornaglia M, Landolfo S, Lembo D. TGF-beta1 and IL-4 downregulate human papillomavirus-16 oncogene expression but have differential effects on the malignant phenotype of cervical carcinoma cells. *Virus Res* 2008; **132**: 253–6.
25 Nindl I, Steenbergen RD, Schurek JO, Meijer CJ, Van der Valk P, Snijders PJ. Assessment of TGF-beta1-mediated growth inhibition of HPV-16- and HPV-18-transfected foreskin keratinocytes during and following immortalization. *Arch Dermatol Res* 2003; **295**: 297–304.
26 Villa LL, Vieira KB, Pei XF, Schlegel R. Differential effect of tumor necrosis factor on proliferation of primary human keratinocytes and cell lines containing human papillomavirus types 16 and 18. *Mol Carcinog* 1992; **6**: 5–9.
27 Vieira KB, Goldstein DJ, Villa LL. Tumor necrosis factor alpha interferes with the cell cycle of normal and papillomavirus-immortalized human keratinocytes. *Cancer Res* 1996; **56**: 2452–7.
28 Woodworth CD, McMullin E, Iglesias M, Plowman GD. Interleukin 1 alpha and tumor necrosis factor alpha stimulate autocrine amphiregulin expression and proliferation of human papillomavirus-immortalized and carcinoma-derived cervical epithelial cells. *Proc Natl Acad Sci U S A* 1995; **92**: 2840–4.
29 Kyo S, Inoue M, Hayasaka N *et al.* Regulation of early gene expression of human papillomavirus type 16 by inflammatory cytokines. *Virol* 1994; **200**: 130–9.
30 Zur Hausen H. Immortalization of human cells and their malignant conversion by high risk human papillomavirus genotypes. *Semin Cancer Biol* 1999; **9**: 405–11.
31 Dong W, Kloz U, Accardi R *et al.* Skin hyperproliferation and susceptibility to chemical carcinogenesis in transgenic mice expressing E6 and E7 of human papillomavirus type 38. *J Virol* 2005; **79**: 14899–908.
32 Galloway DA. Human papillomaviruses: a growing field. *Genes Dev* 2009; **23**: 138–42.
33 Munger K, Howley PM. Human papillomavirus immortalization and transformation functions. *Virus Res* 2002; **89**: 213–28.
34 Takeuchi O, Akira S. Recognition of viruses by innate immunity. *Immunol Rev* 2007; **220**: 214–24.
35 Stanley MA, Pett MR, Coleman N. HPV: from infection to cancer. *Biochem Soc Trans* 2007; **35**: 1456–60.
36 Koromilas AE, Li S, Matlashewski G. Control of interferon signaling in human papillomavirus infection. *Cytokine Growth Factor Rev* 2001; **12**: 157–70.
37 Terenzi F, Saikia P, Sen GC. Interferon-inducible protein, P56, inhibits HPV DNA replication by binding to the viral protein E1. *EMBO J* 2008; **27**: 3311–21.
38 Li S, Labrecque S, Gauzzi MC *et al.* The human papilloma virus (HPV)-18 E6 oncoprotein physically associates with Tyk2 and impairs Jak-STAT activation by interferon-alpha. *Oncogene* 1999; **18**: 5727–37.
39 Ronco LV, Karpova AY, Vidal M, Howley PM. Human papillomavirus 16 E6 oncoprotein binds to interferon regulatory factor-3 and inhibits its transcriptional activity. *Genes Dev* 1998; **12**: 2061–72.
40 Perea SE, Massimi P, Banks L. Human papillomavirus type 16 E7 impairs the activation of the interferon regulatory factor-1. *Int J Mol Med* 2000; **5**: 661–6.
41 Antonsson A, Payne E, Hengst K, McMillan NA. The human papillomavirus type 16 E7 protein binds human interferon regulatory factor-9 via a novel PEST domain required for transformation. *J Interferon Cytokine Res* 2006; **26**: 455–61.

doi: 10.1111/j.1349-7006.2009.01411.x

Virology 406 (2010) 181–188

Contents lists available at ScienceDirect

Virology

journal homepage: www.elsevier.com/locate/yviro

Inhibition of nuclear entry of HPV16 pseudovirus-packaged DNA by an anti-HPV16 L2 neutralizing antibody

Yoshiyuki Ishii [a,*], Keiko Tanaka [b], Kazunari Kondo [c], Takamasa Takeuchi [a], Seiichiro Mori [a], Tadahito Kanda [a]

[a] Pathogen Genomics Center, National Institute of Infectious Diseases, 1-23-1 Toyama, Shinjuku-ku, Tokyo 162-8640, Japan
[b] Department of Pathology, National Institute of Infectious Diseases, 1-23-1 Toyama, Shinjuku-ku, Tokyo 162-8640, Japan
[c] Department of Gynecology and Obstetrics, NTT Medical Center Tokyo, 5-9-22, Higashi-Gotanda, Shinagawa-Ku, Tokyo, 141-8625, Japan

ARTICLE INFO

Article history:
Received 1 April 2010
Returned to author for revision 13 May 2010
Accepted 9 July 2010
Available online 4 August 2010

Keywords:
HPV16
L2
Neutralizing antibody
Anti-P56/75

ABSTRACT

Rabbit anti-HPV16 L2 serum (anti-P56/75) neutralizes multiple oncogenic human papillomaviruses (HPVs). We inoculated HeLa cells with HPV16 pseudovirus (16PV) and with anti-P56/75-bound 16PV (16PV-Ab). Both 16PV and 16PV-Ab attached equally well to the cell surface. However, the cell-attached L1 protein of 16PV became trypsin-resistant after incubation at 37 °C, whereas approximately 20% of the cell-attached 16PV-Ab L1 remained trypsin-sensitive. Confocal microscopy of HeLa cells inoculated with 16PV revealed packaged DNA in the nucleus at 22 h after inoculation; however, nuclear DNA was not detected in cells inoculated with 16PV-Ab. Electron microscopy of HeLa cells inoculated with 16PV showed particles located in multivesicular bodies, lamellar bodies, and the cytosol after 4 h; no cytosolic particles were detected after inoculation with 16PV-Ab. These data suggest that anti-P56/75 inhibits HPV infection partly by blocking viral entry and primarily by blocking the transport of the viral genome to the nucleus.

Introduction

Human papillomavirus (HPV) consists of a double-stranded DNA genome (8 kb) and a non-enveloped icosahedral capsid composed of two capsid proteins, L1 (major) and L2 (minor) (Howley and Lowy, 2001). Based on nucleotide similarities among their L1 genes, HPVs have been classified into more than 100 genotypes. HPV genotype 16 (HPV16) is the most prevalent type linked to cervical cancer worldwide.

HPV propagates only in differentiating keratinocytes (zur Hausen, 2002), which are difficult to culture on a large scale. Hence, it is difficult to prepare HPV virions for detailed studies of the HPV infection process. As a surrogate virus, an infectious HPV pseudovirus, comprising an HPV capsid containing a reporter plasmid, has been developed (Buck et al., 2004). When SV40 T-antigen-positive cells are transfected with expression plasmids for L1 and L2 together with a reporter plasmid carrying SV40-ori, the replicating reporter plasmid is packaged into the capsid formed by the assembly of L1 and L2 in the nucleus, thereby producing pseudovirus (PV). Human cells inoculated with PV express a readily detectable level of the reporter.

Thus far, many studies with PVs have indicated that PV binds to heparin sulfate proteoglycans (HSPGs) on the surface of cells (Giroglou et al., 2001) and then enters the cells by endocytosis mediated by clathrin, caveolin, or the tetraspanin microdomain region (Bousarghin et al., 2003; Day et al., 2003; Hindmarsh and Laimins, 2007; Smith et al., 2008; Spoden et al., 2008). The vesicles containing PV traffic to endosomal compartments, including late endosomes, lysosomes, and cavoesomes (Day et al., 2003; Smith et al., 2008). The mechanisms of viral egress from the organelles and viral uncoating are not clear, but it has been suggested that the minor capsid protein, L2, plays an important role in these events (Day et al., 2004; Kämper et al., 2006; Richards et al., 2006).

L2 is composed of about 470 amino acids. The C-terminal region of L2 binds to L1 (Okun et al., 2001; Finnen et al., 2003). The N-terminal region, with an amino acid sequence that is highly conserved among various HPV types, contains several cross-neutralization epitopes (Pastrana et al., 2005; Kondo et al., 2007). Antiserum obtained from rabbits immunized with a synthetic peptide representing the sequence of HPV16 amino acid residues 56 to 75 (anti-P56/75) neutralizes genotype 16, 18, 31, and 58 PVs (Kondo et al., 2007), as 7well as HPV16 authentic virions produced by raft culture (Conway et al., 2009).

In the present study, we incubated HPV16 PV (16PV) with anti-P56/75 serum or normal rabbit serum and used this to inoculate HeLa cells. We examined the inoculated cells for 16PV attachment to the

* Corresponding author. Fax: +81 3 5285 1166.
E-mail address: yishii@nih.go.jp (Y. Ishii).

0042-6822/$ – see front matter © 2010 Elsevier Inc. All rights reserved.
doi:10.1016/j.virol.2010.07.019

cell surface, internalization of 16PV, and the intracellular localization of 16PV particles and DNA. The results showed that approximately 20% of the antibody-bound 16PV particles failed to enter the cell, and the internalized antibody-bound 16PV particles failed to transport the packaged DNA to the nucleus.

Results

Neutralization of 16PV by anti-P56/75

To examine the effect of anti-P56/75 on pseudoviral infection, HeLa cells were inoculated with 16PV (2.5 μg) preincubated with normal rabbit serum or 16PV (2.5 μg) preincubated with anti-P56/75 serum. After 2 days in culture, cells positive for EGFP were identified by fluorescence microscopy (Fig. 1A) and were counted by fluorescence-activated cell sorting (FACS) (Fig. 1B). Cells inoculated with 16PV preincubated with normal rabbit serum efficiently expressed EGFP (Fig. 1A, upper panel), whereas cells inoculated with 16PV preincubated with anti-P56/75 (1:20 dilution) did not express the reporter protein (Fig. 1A, lower panel). A FACS analysis of 10,000 cells inoculated with 16PV preincubated with normal rabbit serum revealed 6000 EGFP-positive cells (Fig. 1B). In contrast, cells inoculated with 16PV preincubated with anti-P56/75 serum (1:20 dilution) showed almost no EGFP expression by FACS analysis. These data indicate that the incubation of 16PV with anti-P56/75 serum prevented the expression of the PV reporter protein in inoculated cells.

Effect of anti-P56/75 on 16PV attachment to and entry into HeLa cells

To determine the effect of anti-P56/75 on the attachment of 16PV to the cell surface, HeLa cells were incubated with 16PV preincubated with normal rabbit serum or 16PV preincubated with anti-P56/75 serum for 1 h at 4 °C, harvested, lysed, and analyzed by Western blotting with anti-HPV16 L1 monoclonal antibody (Fig. 2A). The antibody recognized similar levels of the L1 virus protein in both cell samples, indicating that the binding of anti-P56/75 to 16PV did not block the attachment of 16PV to the cells.

To investigate the effect of anti-P56/75 on the entry of the virus into cells, HeLa cells inoculated with 16PV preincubated with normal rabbit serum or 16PV preincubated with anti-P56/75 serum were incubated at 37 °C for the indicated times and harvested in the presence or absence of trypsin. After being washed, the cells were lysed and analyzed for the presence of L1 by Western blotting with anti-HPV16 L1 monoclonal antibody (Fig. 2B). In cells without incubation (time 0), L1 was not present in the lysates of cells harvested with trypsin, indicating that L1 had been separated from the cells and digested by trypsin (Supplementary Fig. 1A). Thus, 16PV was still on the surface of the cells before incubation at 37 °C. After 2 h of incubation, some L1 was not digested by trypsin during harvesting

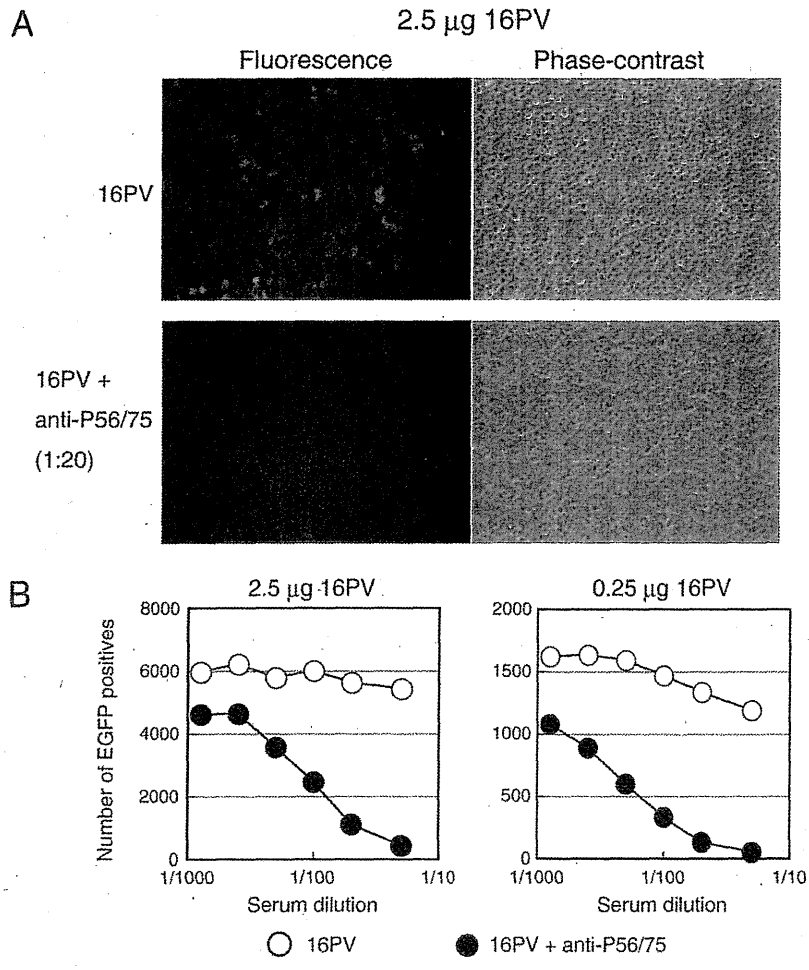

Fig. 1. Neutralization of 16PV by anti-P56/75. The pseudovirus 16PV (2.5 μg or 0.25 μg of L1, as indicated), which carries an expression plasmid for EGFP, was mixed with anti-P56/75 serum or normal rabbit serum in growth medium (500 μl) and incubated at 37 °C for 30 min. HeLa cells were inoculated with the mixture and incubated. After 2 days, the EGFP signal of the cells was observed by fluorescence microscopy (A), and the number of EGFP-positive cells among 10^4 cells was counted by fluorescence-activated cell sorting (FACS) (B). The experiments were performed in duplicate.

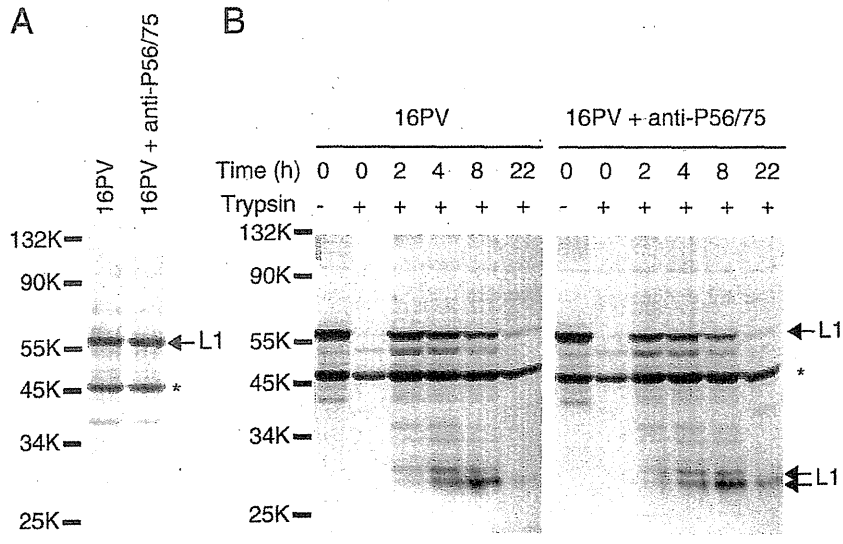

Fig. 2. Attachment and entry of 16PV to HeLa cells. (A) Attachment of 16PV to cells. The 16PV (2.5 μg of L1) was mixed with anti-P56/75 serum or normal rabbit serum (final dilution, 1:20) in growth medium (500 μl) and incubated at 37 °C for 30 min. HeLa cells were inoculated with the mixture and incubated at 4 °C for 1 h. The cells were washed with cold PBS, harvested in PBS containing 2.5 mM EDTA, and then lysed. L1 protein in the lysate was detected by Western blotting with mouse anti-HPV16 L1 antibody. Experiments were performed independently in triplicate. (B) Trypsin resistance of L1. Cells were inoculated and incubated at 4 °C for 1 h as described above. The cells were washed with growth medium and incubated in growth medium at 37 °C for 0, 2, 4, 8, and 22 h. At each time point, the cells were harvested in PBS containing 2.5 mM EDTA (trypsin−) or trypsin (trypsin +) and then lysed. L1 protein in the lysate was detected by Western blotting with mouse anti-HPV16 L1 antibody. Arrows indicate full-sized and degraded L1. Asterisks indicate an unknown protein that reacted with the antibody. Experiments were performed independently in triplicate.

and appeared in the cell lysates, indicating that 16PV had entered the cells. Degraded, smaller L1 fragments appeared in cell lysates at 2 h and became prominent at 4 h. The levels of both intact and degraded L1 were reduced at 22 h, suggesting that L1 was further degraded. The levels of trypsin-resistant L1 in the lysates of cells inoculated with anti-P56/75-bound 16PV (right panel) were approximately 80% of those in lysates of cells inoculated with 16PV in the absence of anti-P56/75 (left panel and Table 1). Thus, approximately 20% of the cell-attached antibody-bound PV failed to enter the cells.

The cells that internalized 16PV in the absence of anti-P56/75 showed reporter protein expression at 2, 4, and 8 h of incubation following inoculation (Supplementary Fig. 1B), indicating that the internalized 16PV was delivered through the infectious pathway.

Effect of anti-P56/75 on the subcellular localization of 16PV L1 and packaged DNA in HeLa cells

To examine the subcellular localizations of 16PV L1 and the DNA packaged inside the capsid, the DNA was labeled by replacing thymidine with 5-ethynil-2′-deoxyuridine (EdU) during replication. EdU-labeled DNA in 16PV lost the ability to express the reporter gene in inoculated 293FT cells (Supplementary Fig. 2). HeLa cells were inoculated with EdU-labeled 16PV preincubated with normal rabbit serum or preincubated with anti-P56/75 serum. The cells were then incubated at 37 °C for the indicated times, fixed with methanol, and fluorescently stained for L1 (Alexa Fluor 555, red signal) and EdU-labeled DNA (Alexa Fluor 488, green signal). Where L1 and the DNA colocalized, the overlapping signals appeared as yellow dots (Fig. 3).

Confocal fluorescence microscopy images show the intracellular localization of L1 and EdU-DNA in HeLa cells inoculated with 16PV preincubated with normal rabbit serum (Fig. 3A, left panel) and in HeLa cells inoculated with 16PV preincubated with anti-P56/75 serum (Fig. 3A, right panel). In each panel, differential interference contrast images are presented to the right of the fluorescence images. The numbers of red, green, and yellow dots at different incubation times are given in Fig. 3B.

In cells inoculated with EdU-labeled PV16 preincubated with normal rabbit serum (Fig. 3A, left panel), capsids with EdU-labeled DNA (yellow dots) and empty capsids or capsids with unlabeled DNA (red dots) were located along the surface of the cells, at a ratio of about 3:2, respectively, before incubation at 37 °C (time 0 h). After incubation at 37 °C for 2 h, some yellow and red dots appeared in the cytoplasm, representing internalization of 16PV. Between 4 and 8 h of incubation, the number of yellow and red dots in the cytoplasm decreased (Fig. 3B). At 22 h, several green dots (approximately 6 ± 3 dots/cell), indicating EdU-labeled DNA that had separated from the capsid, appeared in the nucleus, and some small red dots, representing L1, were seen in the perinuclear region (Figs. 3A and B). Thus, the packaged DNA was released from the capsid and entered the nucleus during incubation at 37 °C.

In cells inoculated with EdU-labeled 16PV preincubated with anti-P56/75 serum, many yellow and red dots were located along the cell surface at time 0 (Fig. 3A, right panel). At 2 h, large yellow dots, which were probably aggregates of 16PV, appeared on the cell surface, where they remained until 22 h. At 22 h, red dots were observed in the perinuclear region, but no green dots were ever present in the nucleus (Figs. 3A and B).

Table 1
Percentage of trypsin-resistant L1[a].

	Incubation at 37 °C	
	2 h	4 h
16 V	64.3 (16.5)	64.9 (3.71)
16 V + anti-P56/75	52.1 (17.1)	53.9 (9.13)

Results are presented as average percentage of three independent experiments (standard deviation).
[a] Cell-attached L1 at 0 h was set to 100%.

Effect of anti-P56/75 on the subcellular localization of 16PV particles in HeLa cells

The subcellular localization of 16PV particles in HeLa cells was studied using transmission electron microscopy (Fig. 4). HeLa cells were inoculated with 16PV preincubated with normal rabbit serum or

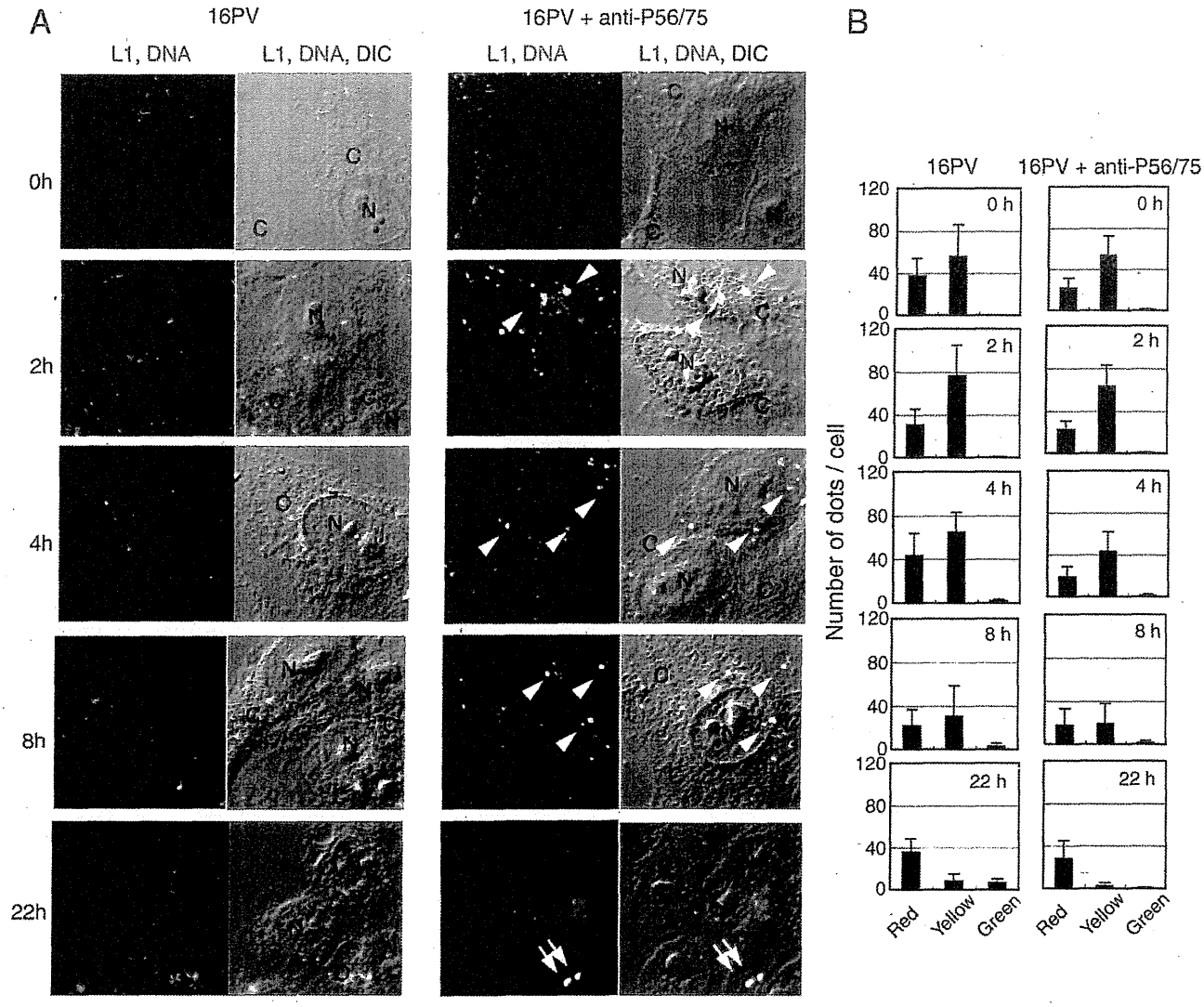

Fig. 3. Subcellular localization of L1 protein and packaged DNA. (A) The 16PV (2.5 μg of L1) containing 5-ethynil-2′-deoxyuridine (EdU)-labeled DNA was preincubated with anti-P56/75 serum (final dilution, 1:20) or normal rabbit serum in growth medium (500 μl) at 37 °C for 30 min and used to inoculate HeLa cells. The cells were incubated at 4 °C for 1 h, washed with growth medium, incubated in growth medium at 37 °C for 0, 2, 4, 8, and 22 h, fixed with methanol, and fluorescently labeled for L1 (Alexa Fluor 555, red dots) and EdU-labeled DNA (Alexa Fluor 488, green dots). Colocalized L1 and DNA appear as yellow dots. Confocal fluorescence microscopy images of cells inoculated with 16PV in the absence (left panel) and presence of anti-PV56/75 (right panel) are presented, along with the differential interference contrast images. The small arrowheads indicate a large aggregate of antibody-bound 16PV particles; thought to be on the cell surface. The arrows indicate an aggregate that appears to be at the contact site between two adjacent cells. Experiments were performed twice independently. N: nucleus, C: cytoplasm. (B) Numbers of red, yellow, and green dots in the cells. Red (L1), yellow (L1 and DNA), and green (DNA) dots were counted in 20 randomly selected cells of the indicated samples. Error bars represent the standard deviation.

16PV preincubated with anti-P56/75 serum. HeLa cells in the absence of 16PV served as a control. After a 4-h incubation, the cells were fixed and embedded. Ultra-thin sections (70 nm) were cut, stained with 4% uranyl acetate, and viewed under a transmission electron microscope.

HeLa cells incubated with either 16PV preparation showed particles with an approximate diameter of 55 nm on their surface (Figs. 4B and C). The electron-dense particles were probably capsids containing DNA, as these particles were not detected on the cells incubated without 16PV (Figs. 4A and E). The particles of antibody-bound 16PV formed a large aggregate (Fig. 4C), but no particle aggregation was detected in the cells inoculated with 16PV in the absence of antibody (Fig. 4B). This result is consistent with the confocal microscopy images of the cells at 2 and 4 h. The aggregate was likely unable to enter the cell and remained on the cell surface.

The particles of 16PV were located in multivesicular bodies (MVBs; 200–500 nm and 500–1,000 nm in diameter), which are late endosomes containing multiple lumenal vesicles; in lamellar bodies (LBs), which are lysosomal organelles containing multiple concentric membrane layers (Schmitz and Müller, 1991); in lysosome-like MVBs (L-MVBs), which are relatively electron-dense organelles; and in the cytosol (Figs. 4D and F, capsids are indicated by arrows). There were fewer particles of antibody-bound 16PV, and these were located in MVBs and L-MVBs, but not in the large MVBs (500–1000 nm in diameter) or the cytosol (Table 2). Some 16PV particles were attached to the limiting membrane of MVBs (Fig. 4F), whereas no particles of antibody-bound 16PV were attached to the membrane (Fig. 4G). These observations suggest that any antibody-bound 16PV that entered the cell did not egress from the endosomal compartments.

Discussion

In the present study, the binding of anti-P56/75 to 16PV did not affect the attachment of 16PV to HeLa cells, as shown by Western blot analysis of cell lysates and by confocal fluorescence microscopy. In

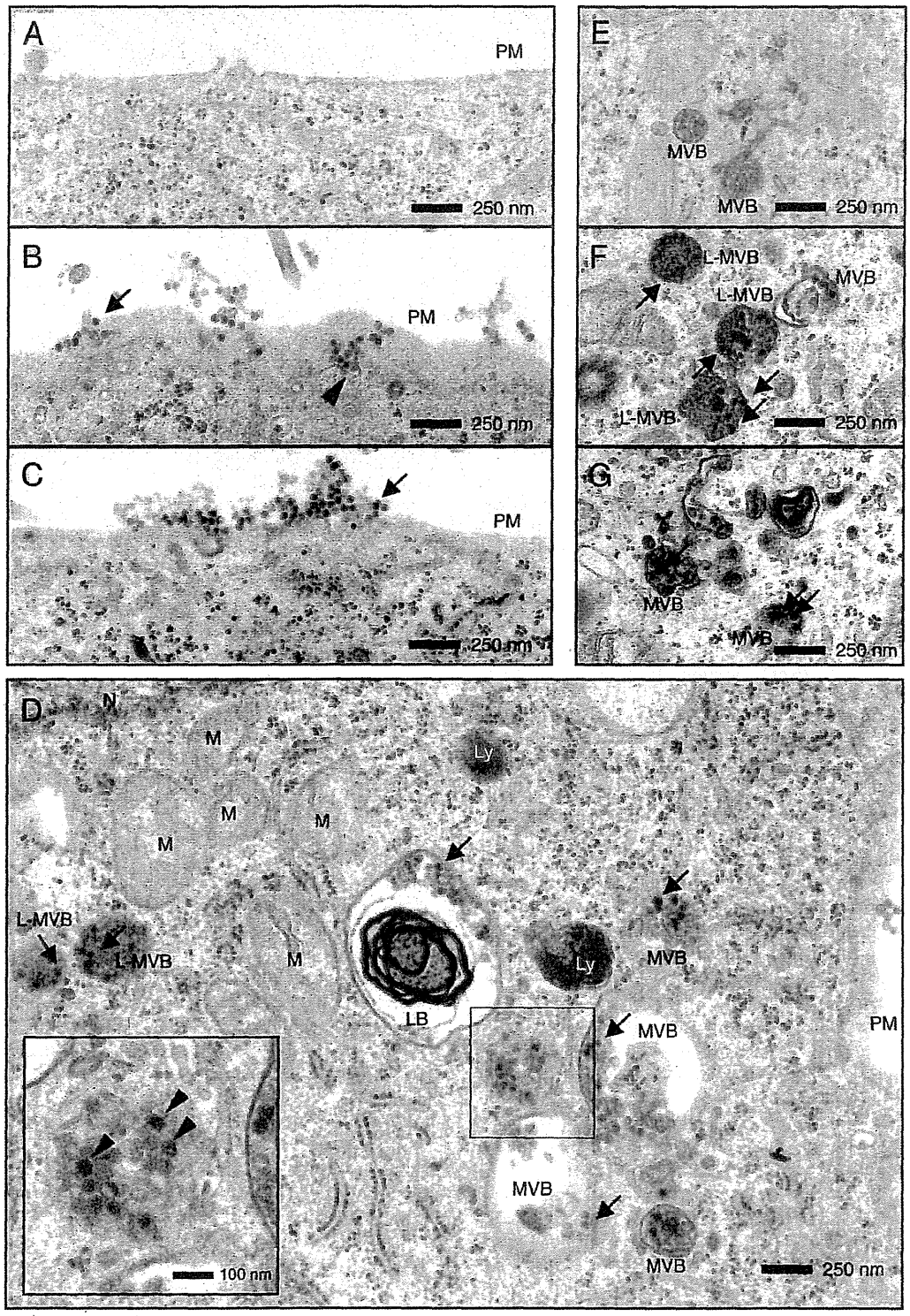

Fig. 4. Subcellular localization of 16PV particles. The 16PV (10 μg of L1) was mixed with anti-P56/75 serum or normal rabbit serum (final dilution, 1:10) in growth medium (1 ml) and incubated at 37 °C for 30 min. HeLa cells (6×10^5) were inoculated with the mixture, incubated at 37 °C for 4 h, fixed, and embedded. Ultra-thin sections were cut and stained with uranyl acetate for observation by transmission electron microscopy. A and E: Cells were not inoculated with 16PV. B, D, and F: Cells were inoculated with 16PV preincubated with normal rabbit serum. C and G: Cells were inoculated with 16PV preincubated with anti-P56/75 serum. Arrows in B and C indicate particles on the cell surface. The arrowhead in B indicates an invagination of the plasma membrane. The arrows in D indicate particles in endosomal compartments (MVBs, LBs, and L-MVBs); cytosolic particles are boxed, and an enlargement is shown in the inset. The arrows in F indicate particles located near the limiting membranes of L-MVBs. The arrow in G indicates particles in MVBs. Experiments were performed twice independently. LB: lamellar body; L-MVB: lysosome-like multiple vesicular body; Ly: lysosome; M: mitochondrion; MVB: multiple vesicular body; N: nucleus; PM: plasma membrane.